



Constraints on the carbon cycle from the NASA Carbon Monitoring System

Kevin W. Bowman

Jet Propulsion Laboratory

California Institute of Technology



CMS team:

Kevin Bowman, Junjie Liu, Nicholas Parazoo, Meemong Lee, Dimitris Menemenlis, Holger Brix, Joshua Fisher, Christian Frankenberg

Jet Propulsion Laboratory, California Institute of Technology

**Joint Institute for Regional Earth System Science and Technology, University of California,
Los Angeles**

Steven Pawson, Lesley Ott, James Collatz, Watson Gregg, Zhengxin Zhu,
Randy Kawa, Cecile Rousseaux

NASA Goddard Space Flight Center

Chris Hill, Mick Follows, Stephanie Dutkiewicz

MIT

Scott Denning, Kathy Haynes, Ian Baker

Colorado State University

Kevin Gurney

Arizona State University

Gregg Marland, Eric Marland, Chris Badurek

Appalachian State University

Daven Henze and Nicholas Bouserez

University of Colorado, Boulder



Milestone in Climate Forcing



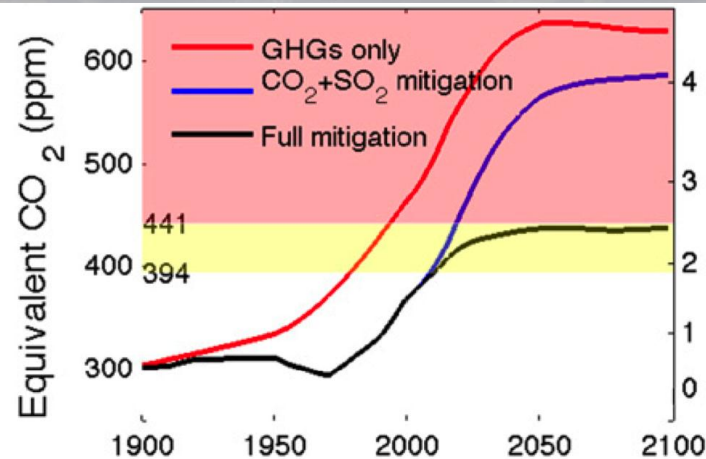
Continuing reliance on coal, which fuels this power plant in Germany, is driving carbon dioxide levels in the atmosphere ever higher.

CLIMATE

Global carbon dioxide levels near worrisome milestone

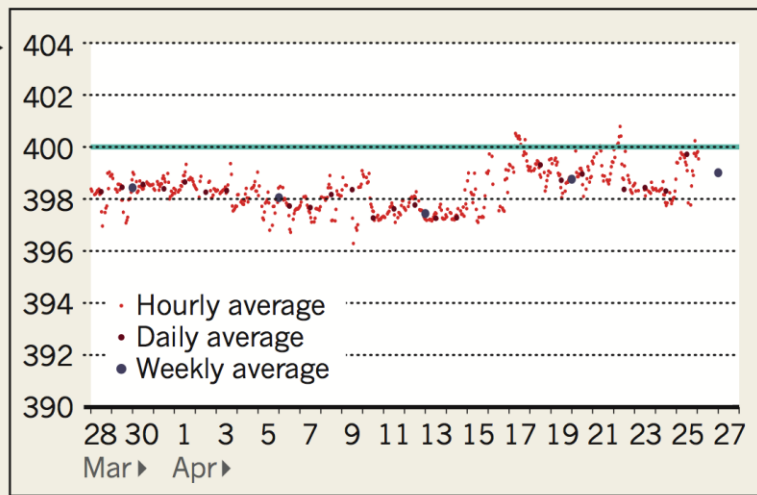
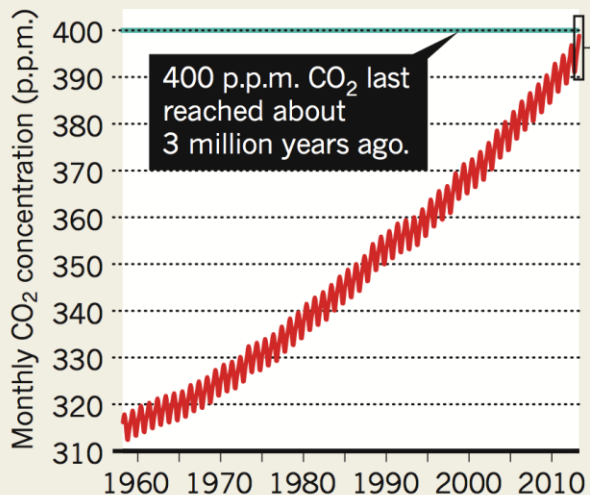
Concentrations of greenhouse gas will soon surpass 400 parts per million at sentinel spot.

We are entering into the world of “dangerous climate change”



ON THE RISE

Measurements of atmospheric CO₂ levels at Mauna Loa, Hawaii, show that the greenhouse gas has accumulated steadily, and spiked above 400 parts per million (p.p.m) several times in April.



14 | NATURE | VOL497 | 2MAY2013

Ramanathan and Xu, PNAS (2010)



Multi-scale mitigation efforts

UN-REDD PROGRAMME

The United Nations Collaborative Programme on Reducing Emissions from Deforestation and Forest Degradation in Developing Countries



California AB-32

NEWS IN FOCUS



Cities such as Los Angeles produce plumes of pollution that contain greenhouse gases.

Nature, Dec. 2012

CLIMATE CHANGE

Megacities move to track emissions

Scientists monitor greenhouse gases in urban areas as a first step to gauging success of climate initiatives worldwide.

California Environmental Protection Agency
Air Resources Board

Home | Reducing Air Pollution | Air Quality | Business Assistance | Laws & Regulations | Health

A Clean Energy Jobs Plan

An eight-point action plan for investment in renewable energy technology and the creation of more than half a million green jobs

California's Clean Energy Future

- Governor Jerry Brown - Clean Energy Jobs Plan
- New Vision for California's Clean Energy Future
- Setting the Record Straight on AB 32
- What They're Saying...About AB 32, Clean Energy

VIDEOS

- The Road to Clean Energy
- Energy Makeover
- CLIMATE PLAN

Independent efforts are being made to help mitigate climate change



A changing carbon cycle

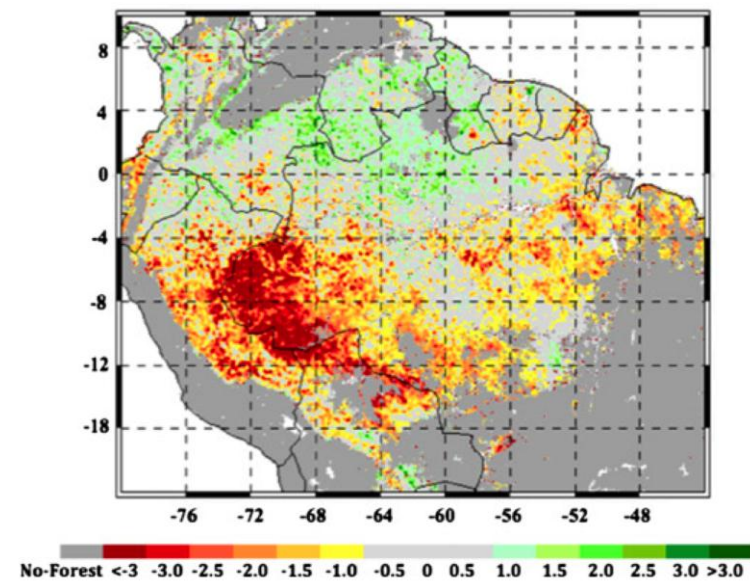
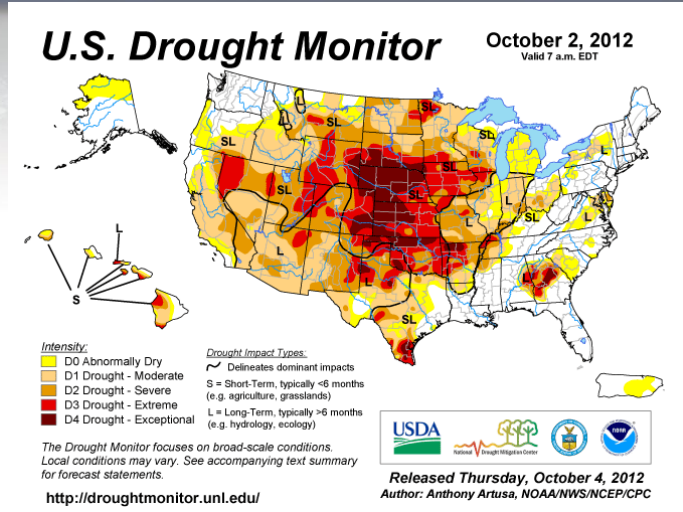
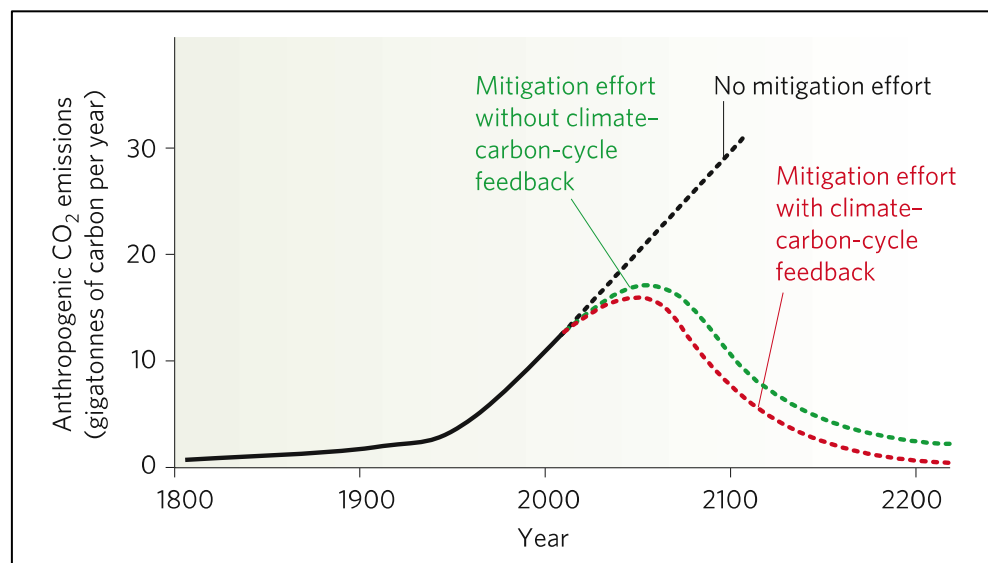
A steep road to climate stabilization

Pierre Friedlingstein

The only way to stabilize Earth's climate is to stabilize the concentration of greenhouse gases in the atmosphere, but future changes in the carbon cycle might make this more difficult than has been thought.

Science, 2008

Changes in the physical climate may undermine the ability of the natural carbon cycle to partially sequester atmospheric CO₂



Saatchi et al, PNAS, 2013

NASA Carbon Monitoring System



<http://carbon.nasa.gov>



The objective of the NASA CMS Flux Project is to incorporate the full suite of NASA observational, modeling, and assimilation capabilities to attribute climate forcing to spatially resolved surface fluxes across the entire carbon cycle.

**“Bottom-up”
Satellite data**

**“Bottom-up”
assimilation/models**

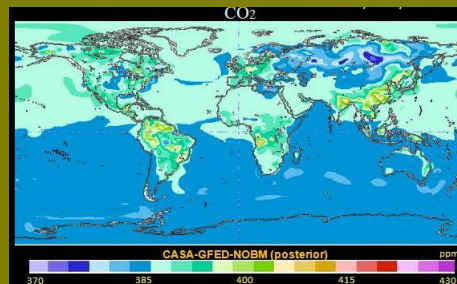
GEOS-Chem CO₂ transport model



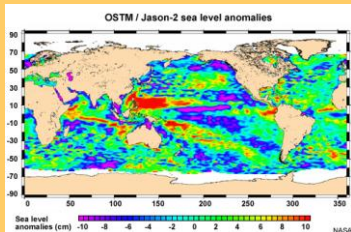
Land Surface data
(fPar, EVI, etc)

Land
CASA/
CASA-
GFED/Si
b4/
MsTMIP

GPP, Rh,
BB
 x_a, S_a



Meteorology
GEOS-5



Ocean data
(chlorophyll,
salinity, etc)

Ocean
NOBM/E
CCO2-
Darwin

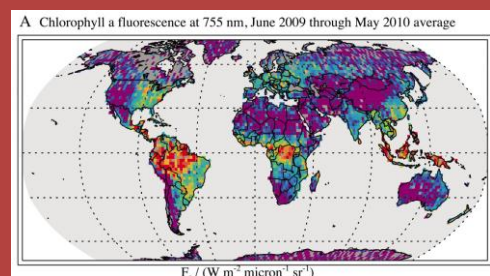
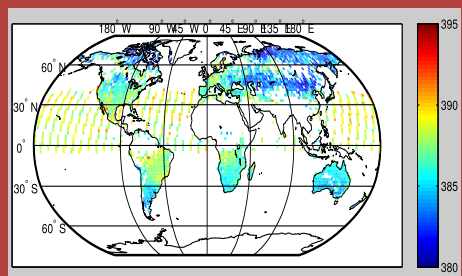
ASE

“Top-down” inverse model

$$\min_{\mathbf{x}_0} C(\mathbf{x}) = \left\{ \sum_i (\mathbf{y}_i - \mathbf{F}_i(\mathbf{x}))^\top (\mathbf{S}_i^n)^{-1} (\mathbf{y}_i - \mathbf{F}_i(\mathbf{x})) + (\mathbf{x}_0 - \mathbf{x}_a)^\top \mathbf{S}_a^{-1} (\mathbf{x}_0 - \mathbf{x}_a) \right\}$$

new satellite data

ACOS-GOSAT/OCO-2 xCO₂ GOSAT fluorescence



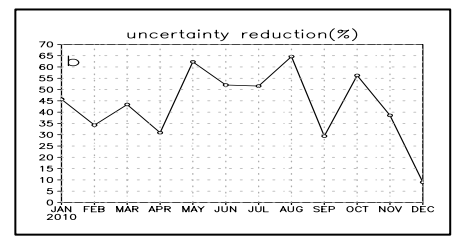
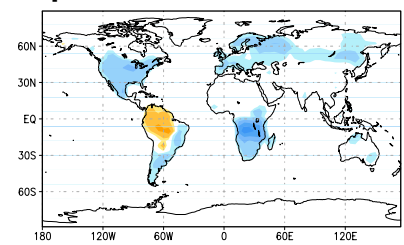
Fossil fuel
emissions: FF



“Top-down” flux estimates and uncertainties

Human
FFDAS

$\hat{\mathbf{x}}, \hat{\mathbf{S}}$



Anthropogenic
data (nightlights)

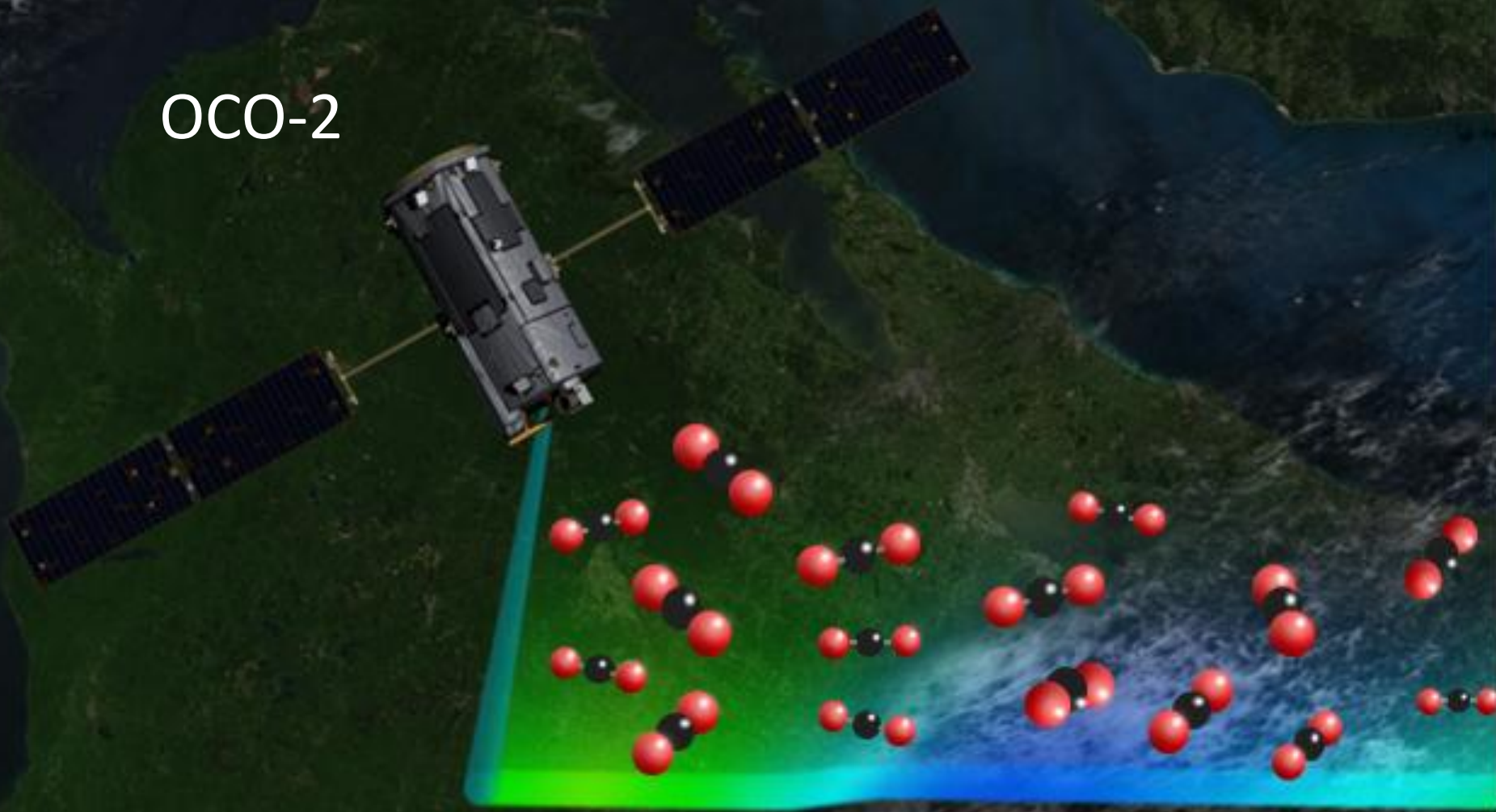
$GPP^{\hat{}}$, \hat{R}_h , $ASE^{\hat{}}$, $FF^{\hat{}}$, $BB^{\hat{}}$



Observations of xCO₂ from space-

The NASA Orbiting Carbon Observatory-2 (OCO-2) and JAXA-GOSAT Mission

OCO-2





Measuring CO₂ from Space

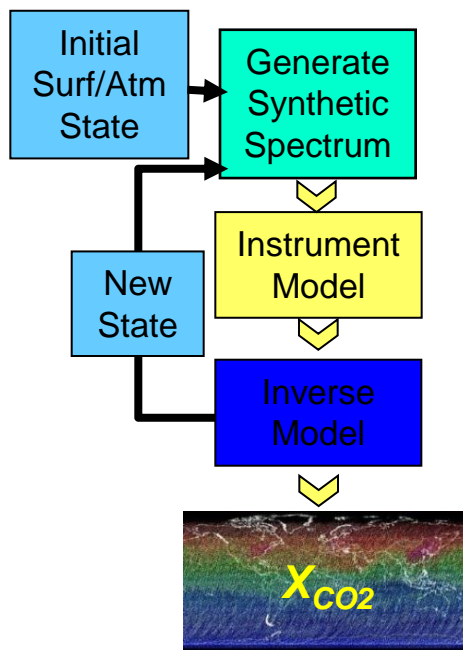
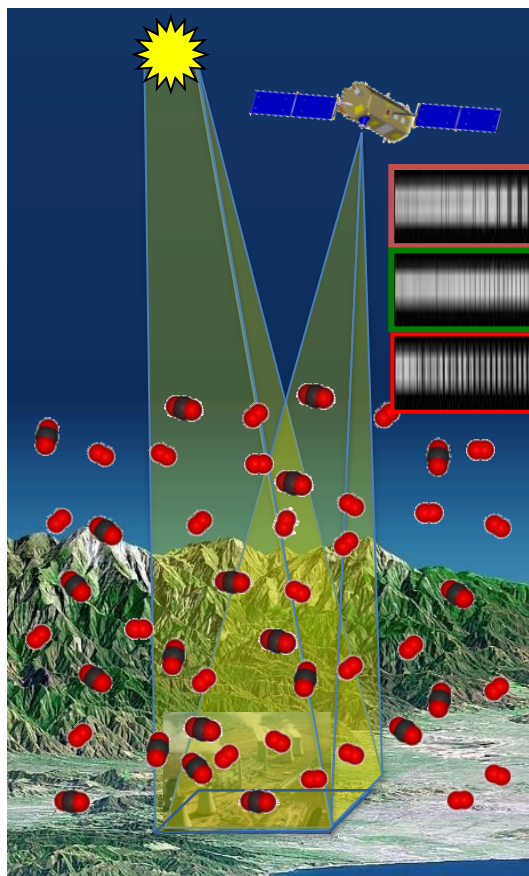
- Record spectra of CO₂ and O₂ absorption in reflected sunlight



- Retrieve variations in the *column averaged CO₂ dry air mole fraction, X_{CO2}* over the sunlit hemisphere



- Validate measurements to ensure X_{CO2} accuracy of 1 - 2 ppm (0.3 - 0.5%)





Attribution Strategy

A priori carbon cycle budgets are constructed to be consistent with atmospheric CO₂ growth

10.1 GtC ± 0.5 GtC



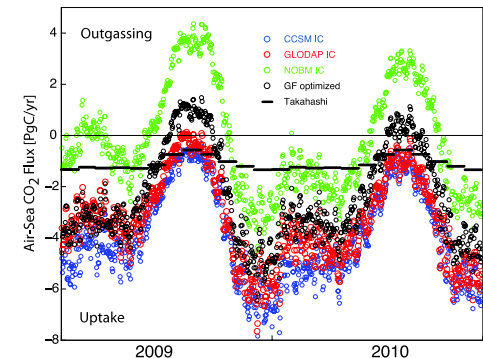
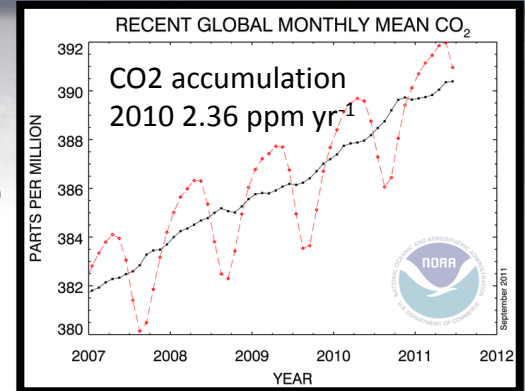
Fossil Fuel+Land Use Change
(CDIAC+Global Carbon Project 2010)
Incorporates chemical CO₂ production
aviation, bunker, and shipping
(Nassar et al, 2010)

5.0 ± 0.2 PgC y⁻¹
50%

2.6 ± 1.0 PgC y⁻¹
26%

Calculated as the residual
of all other flux components

2.4 ± 0.5 PgC y⁻¹
24%
Derived from ECCO-2 ocean flux estimate



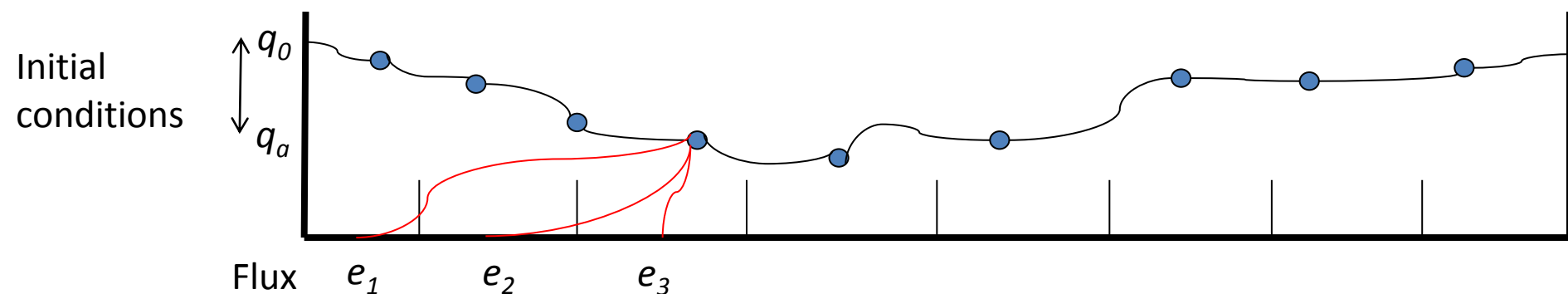


4D-var assimilation approach

$$\min_{\mathbf{x}_0} C(\mathbf{x}) = \left\{ \sum_i (\mathbf{y}_i - \mathbf{F}_i(\mathbf{x}))^\top (\mathbf{S}_n^i)^{-1} (\mathbf{y}_i - \mathbf{F}_i(\mathbf{x})) + (\mathbf{x}_0 - \mathbf{x}_a)^\top \mathbf{S}_a^{-1} (\mathbf{x}_0 - \mathbf{x}_a) \right\}$$

subject to $\mathbf{x}_{i+1} = \mathbf{M}_i(\mathbf{x}_i, \mathbf{p}_i)$

State vector $\mathbf{x} = \begin{bmatrix} \mathbf{q} \\ \mathbf{e} \end{bmatrix}$



- Both an initial condition and boundary condition problem
- Initial conditions solved through “sliding window” technique from Feng and Jones (UT)
- Monthly NEE estimated over a year window.
- Estimate of terrestrial flux **only**

4D-var

\mathbf{x} : monthly scale factor

$[\mathbf{S}_a]_{ii}$ = CASA-GFED3 Monte Carlo

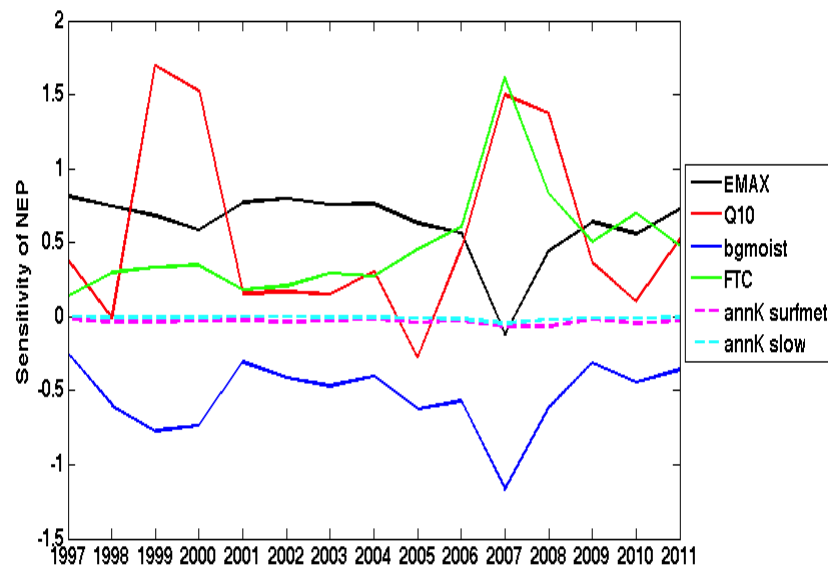
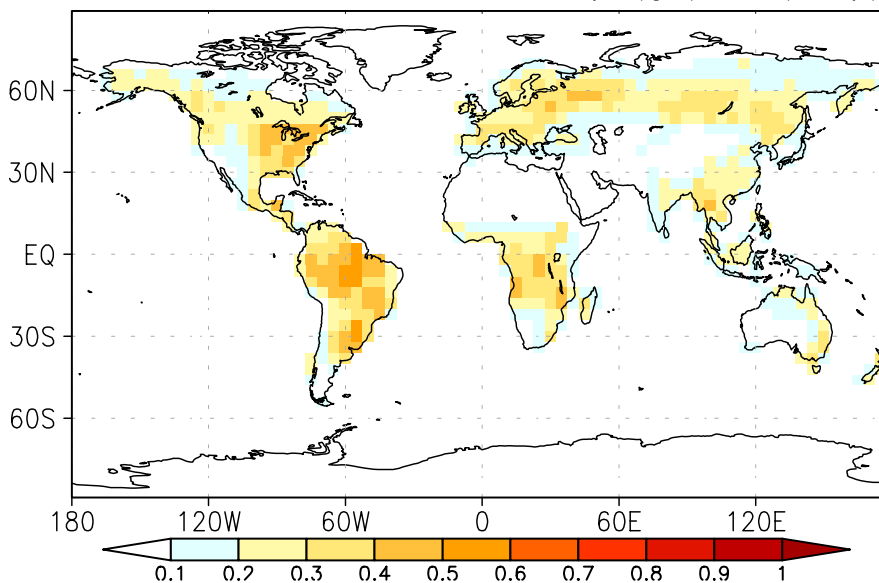
\mathbf{S}_n = Observational error from ACOS. No transport error or horizontal correlation error.



CASA-GFED3 terrestrial eco-system model

- The CASA-GFED3 model is modified to have an annual flux consistent with the inferred terrestrial flux.
- Spatial uncertainties are estimated through a Monte Carlo analysis through perturbation of key environmental parameters such as maximum potential light use efficiency, Q10, forest tree cover, etc.
 - Quantifies parameteric uncertainty (but not structural uncertainty)

annual mean CASA uncertainty (gC/m²/day)

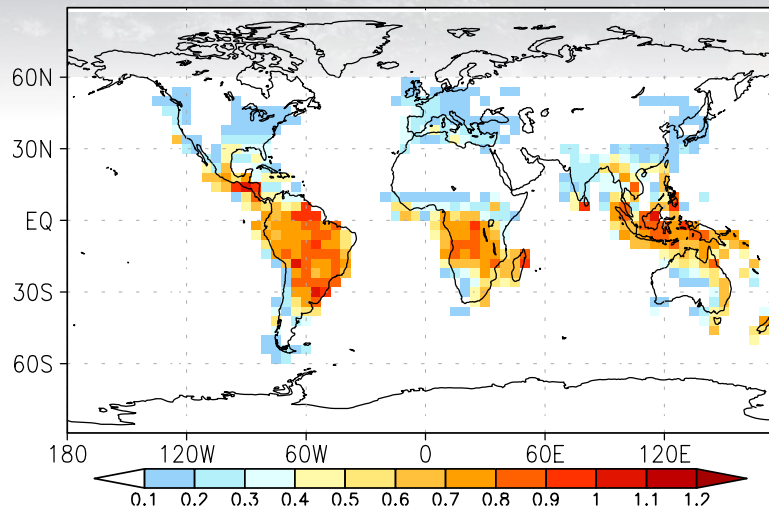


Interannual sensitivity of global *NEP* (no fire) to selected CASA-GFED parameters.

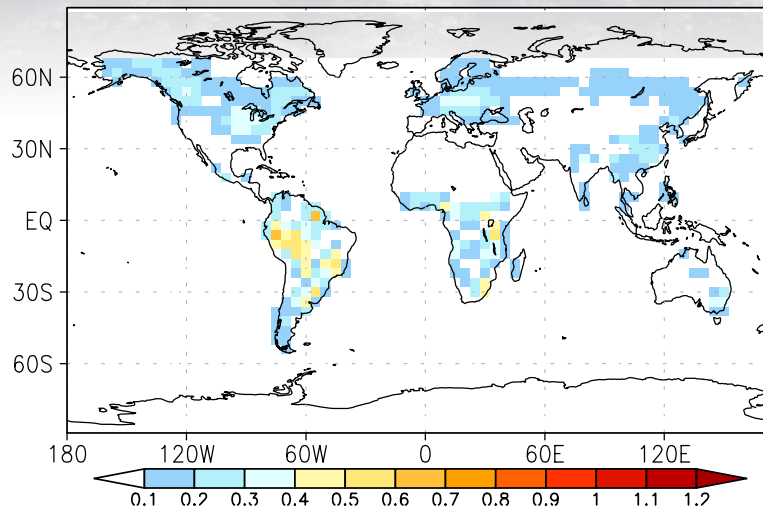


CASA-GFED NEE uncertainty: role of the tropics

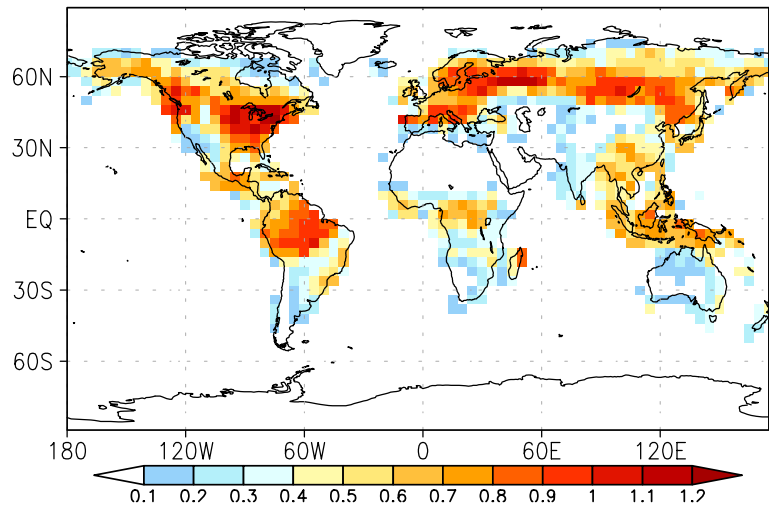
CASA uncertainty (gC/m²/day), Feb



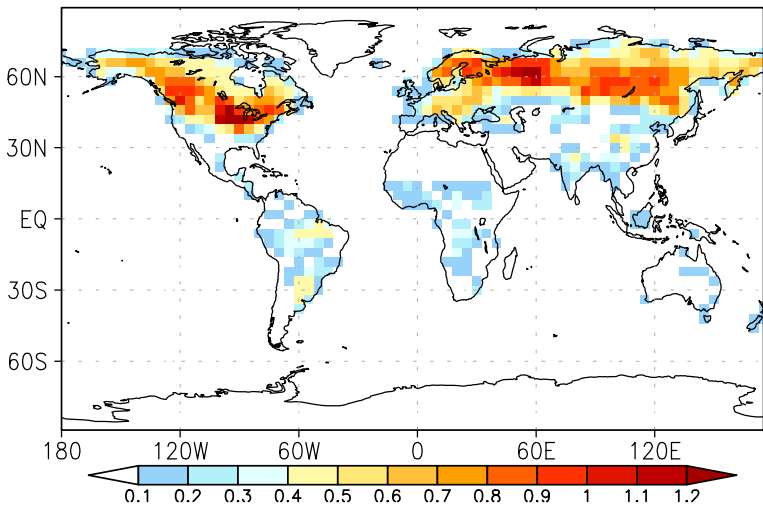
50%



CASA uncertainty (gC/m²/day), July

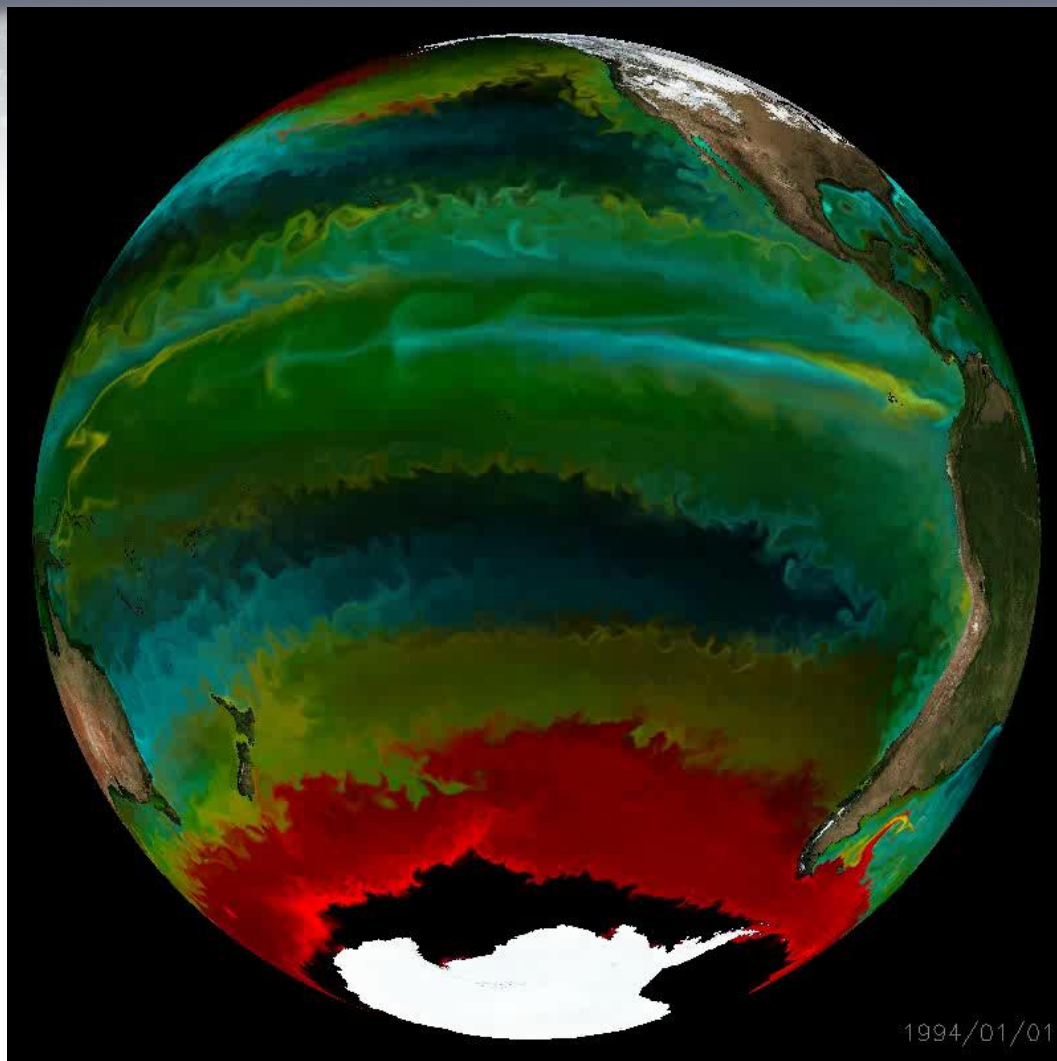


50%





ECCO2-Darwin ocean biogeochemical model



Concentration of different species categories
Diatoms (red), Prochlorococcus (green)
Picoplankton (blue), Everything else (yellow)

ECCO2: Eddying Global-Ocean and Sea-Ice Data Synthesis

18 km-cubed sphere, physical ocean 4D--
-variational assimilation

(Menemenlis et al, 2008)

Darwin: Ocean Biogeochemistry (Follows et al., 2007)

Biogeochemistry is constrained by a Green's function approach (least squares)

Model: $y - G[x_b] \approx G(x - x_b) + n$

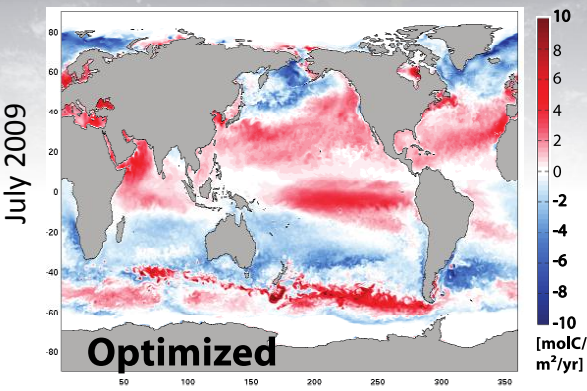
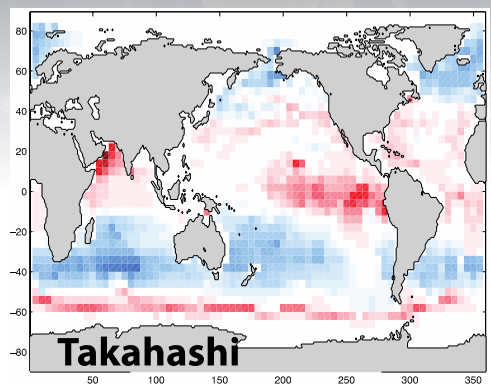
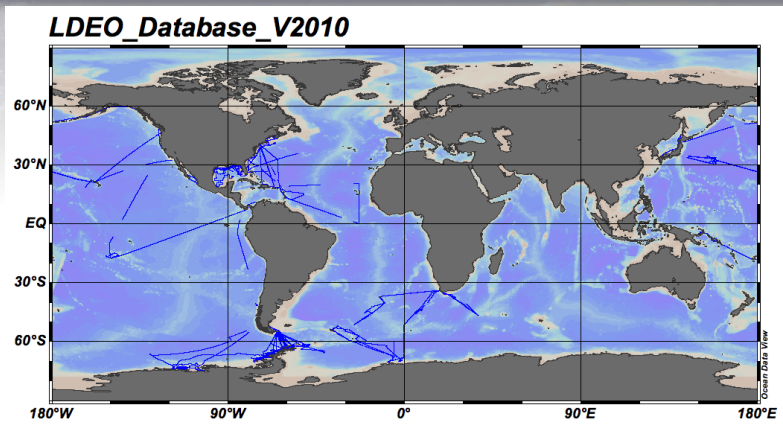
Solution:

$$x = x_b + (G^T G)^{-1} G^T (y - G[x_b])$$

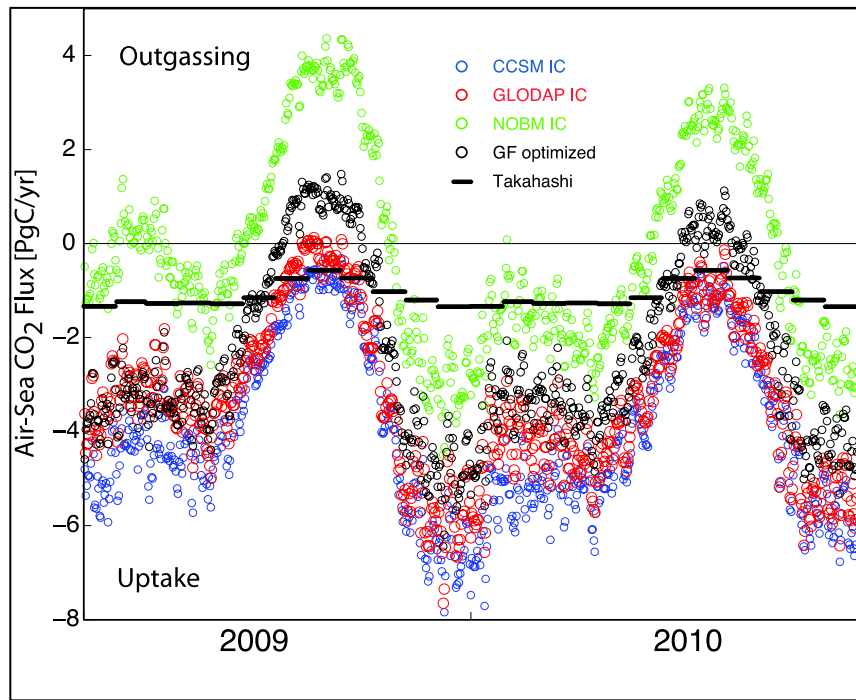
G is a kernel matrix whose columns are computed using a GCM sensitivity experiment for each parameter in vector **x**, which are the initial conditions. Subscript "b" represents baseline GCM integration used to linearize problem.



Preliminary assimilation of LDEO pCO₂, 2009-2010



Seven ECCO2-Darwin sensitivity integrations differing in their initial conditions (IC) for dissolved inorganic carbon (DIC), alkalinity (Alk), and oxygen and in biogeochemical parameterizations were used for the optimization.



Simulated mean air-sea CO₂ fluxes during 2009-2010 in PgC/yr:

NOBM IC: -0.2

Takahashi: -1.1

Optimized: -2.4

GLODAP IC: -3.5

CCSM IC: -4.0

Brix *et al*, in preparation (2013)

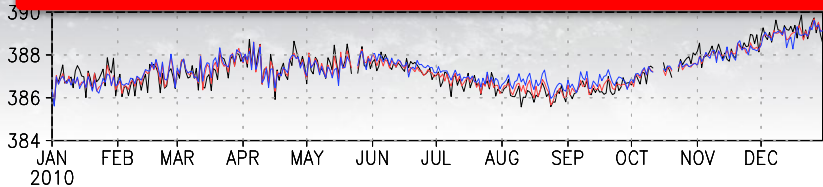


Comparison of CMS-Flux to GOSAT

ACOS: black: prior: blue: post: red

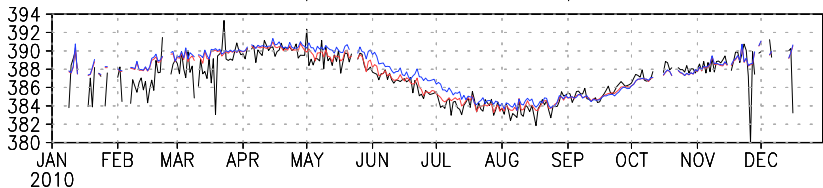
obs=387.302,post=387.305,prior=387.383

- CMS-Flux total annual flux agrees with GOSAT to within 0.01 ppm.
- Zonal and seasonal differences range from 0.5 to 1 ppm

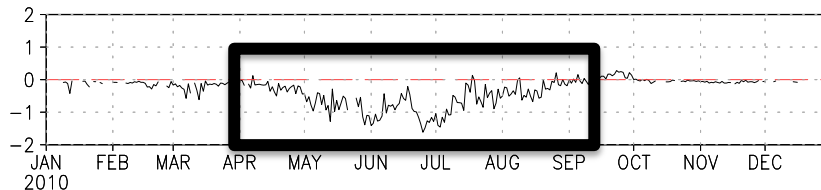


lon0-lon360,lat40-lat60

obs=387.123,post=387.496,prior=387.804

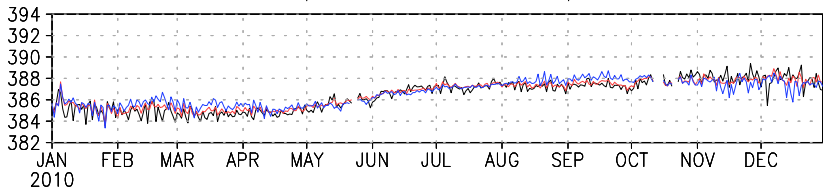


lon0-lon360,lat40-lat60

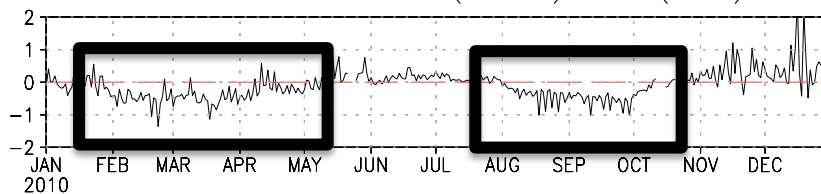


lon0-lon360,lat(-40)-lat(-6)

obs=386.467,post=386.565,prior=386.653

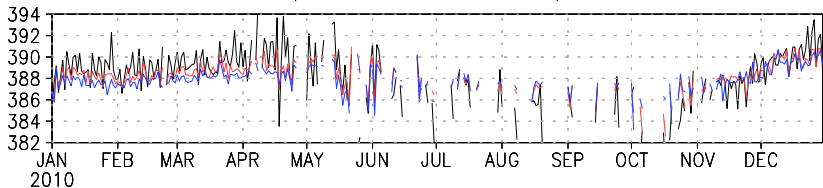


lon0-lon360,lat(-40)-lat(-6)

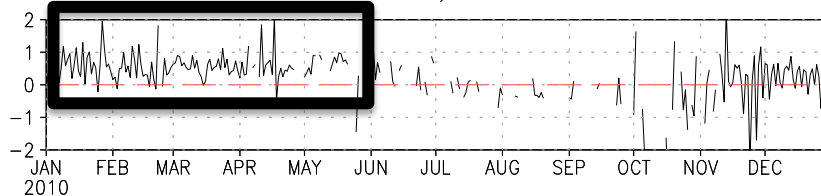


lon0-lon360,lat-6-lat14

obs=388.21,post=388.165,prior=387.881



lon0-lon360,lat-6-lat14

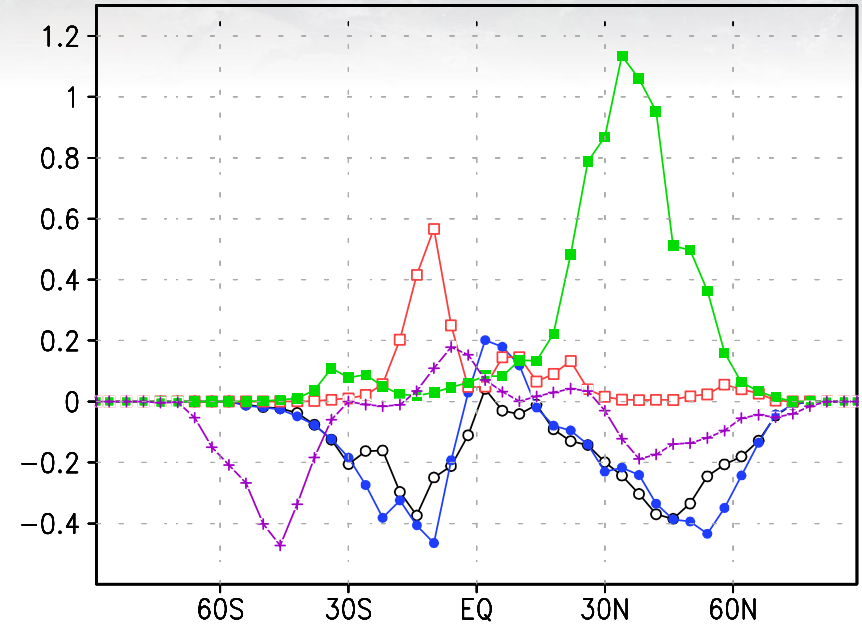
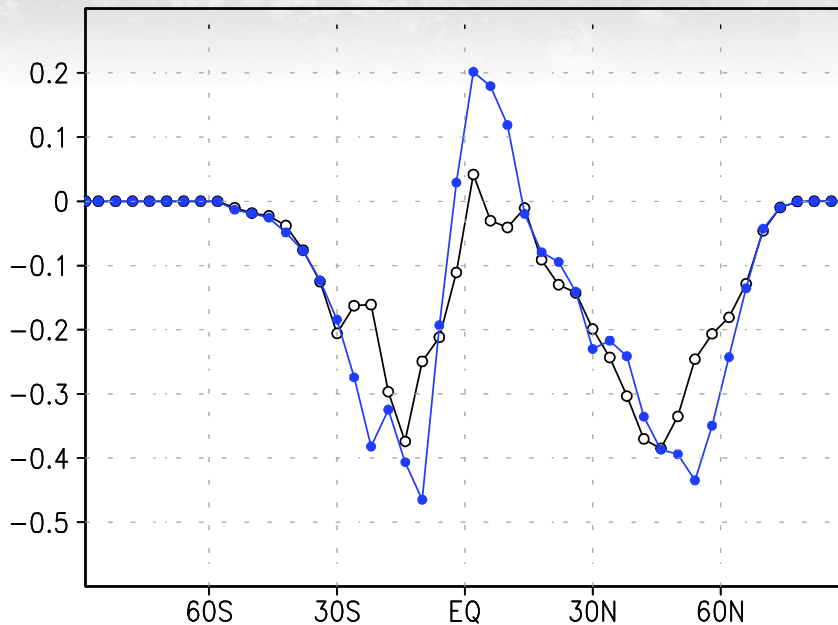




Posterior flux estimate 2010

Prior flux=-5.12GtC, posterior flux=-5.36GtC

Black: prior; blue: posterior; green: fossil fuel; red: biomass burning; purple: ocean flux



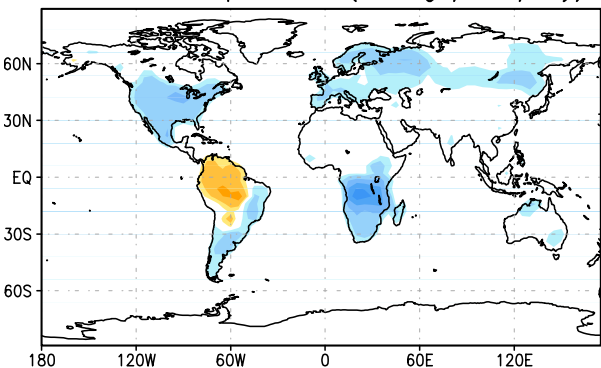
- Prior flux (Black); Posterior flux (blue)
- Posterior estimate redistributes the flux meridionally.
- The posterior flux increases carbon uptake over the NH mid-latitude and SH subtropics while reducing uptake over the tropics relative to the prior carbon budget.
- It's important to remember that $x\text{CO}_2$ is only sensitivity to the total flux. Uncertainties in one part of the carbon cycle can alias into the other.



Spatial attribution of CO₂

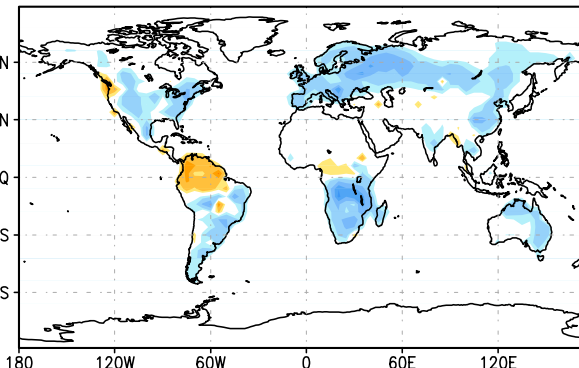
Annual mean prior flux (gC/m²/day)

annual mean prior flux (unit: gC/m²/day)



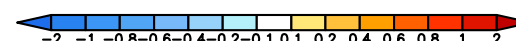
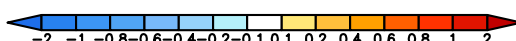
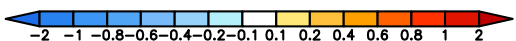
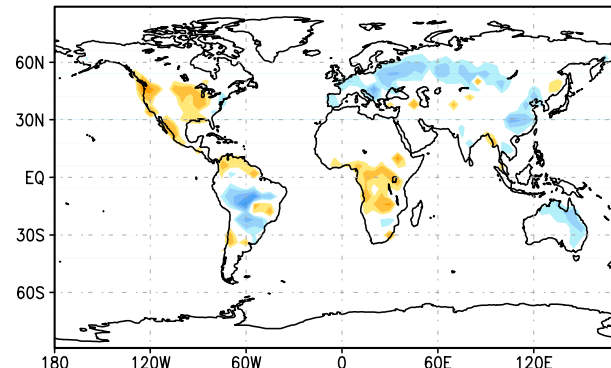
Annual mean posterior flux (gC/m²/day)

annual mean posterior flux
newB (unit: gC/m²/day)



Post-prior (gC/m²/day)

annual mean (post(newB)-prior)
flux (unit: gC/m²/day)

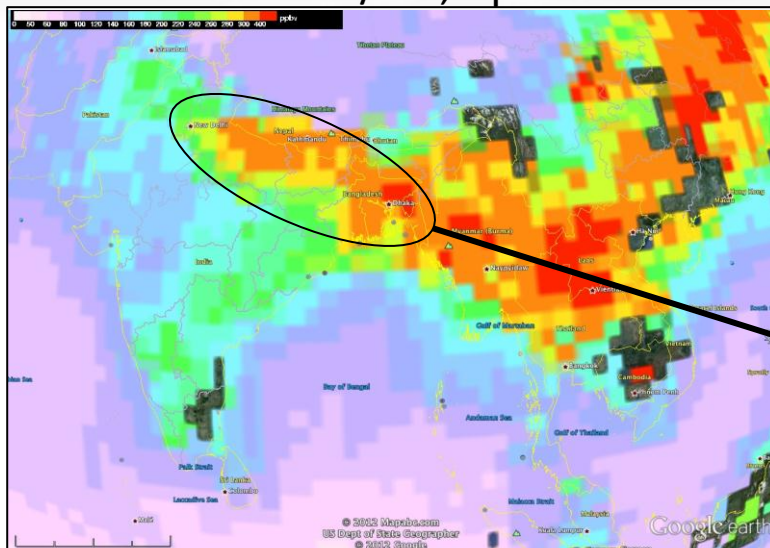


- Zonal redistribution of carbon uptake in the Northern Hemisphere between Europe (stronger) and North America (weaker)
- Zonal redistribution in the tropics with reduced uptake in Africa but increased uptake in the Amazon

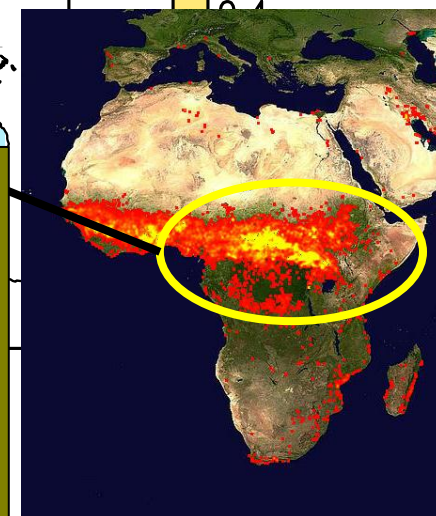
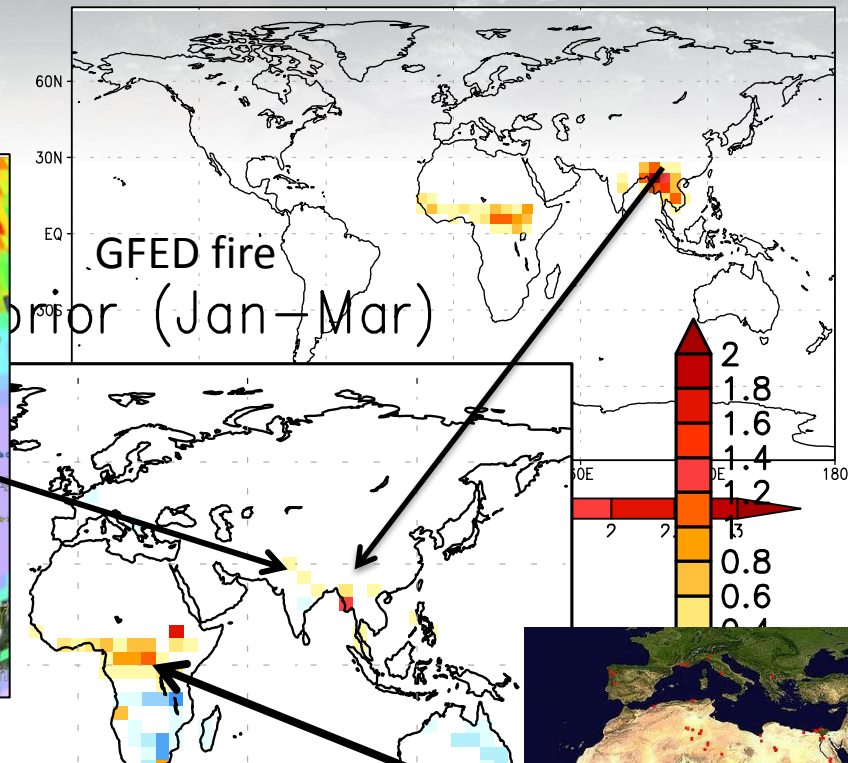


Anthropogenic emissions and Biomass burning

MOPITT V5 NIR/TIR, April 2010



January–Mar



Kar *et al*, ACP 2010 showed elevated, CO, AOD and ozone have been observed from space in the Eastern Indo-Gangetic Planes.

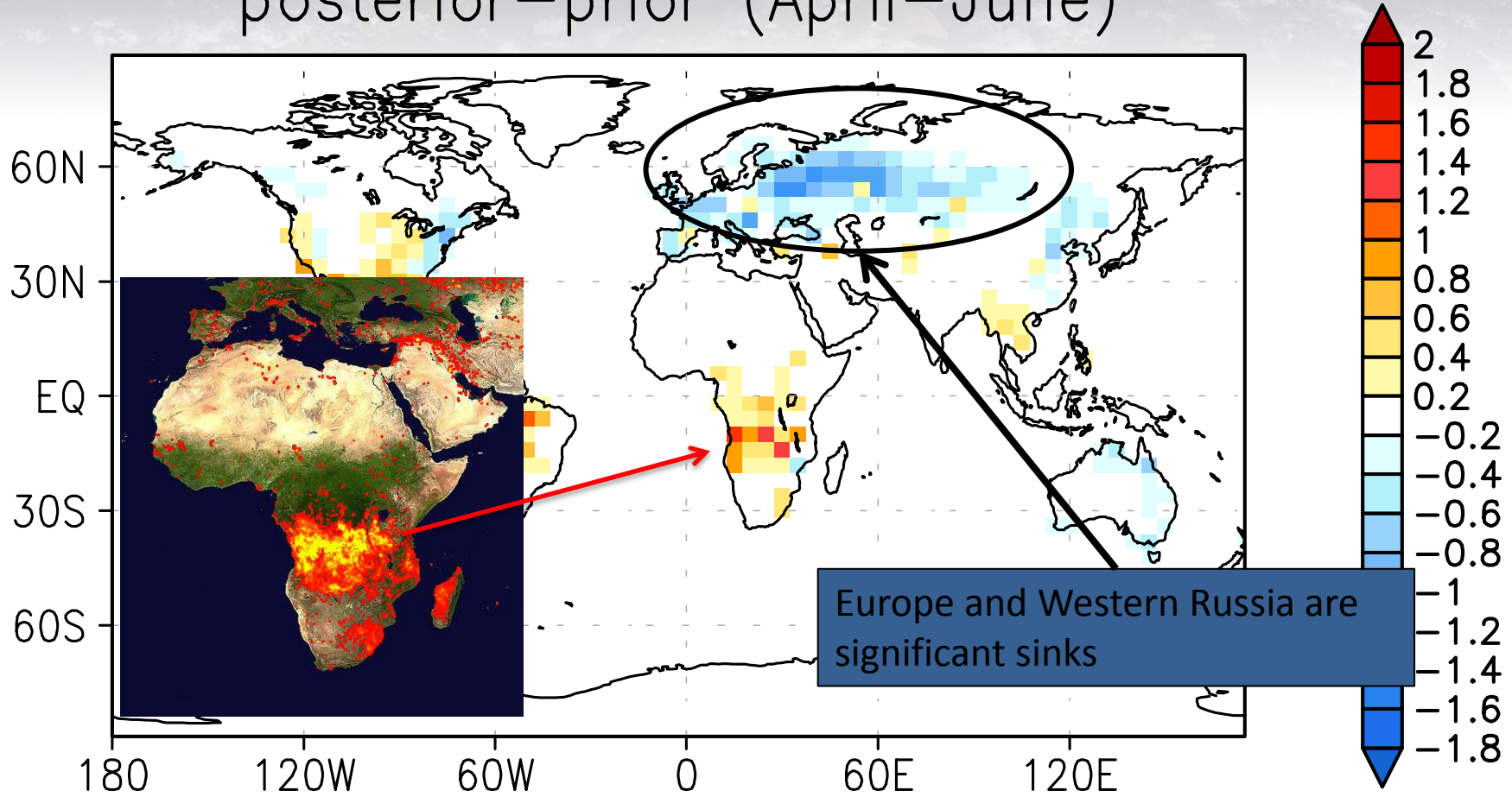
Elevated CO₂ in Southeast Asia is broadly consistent with enhanced CO and GFED patterns.

Elevated CO₂ in Africa north of the ITCZ consistent with MODIS firecounts.



European sink and African biomass burning

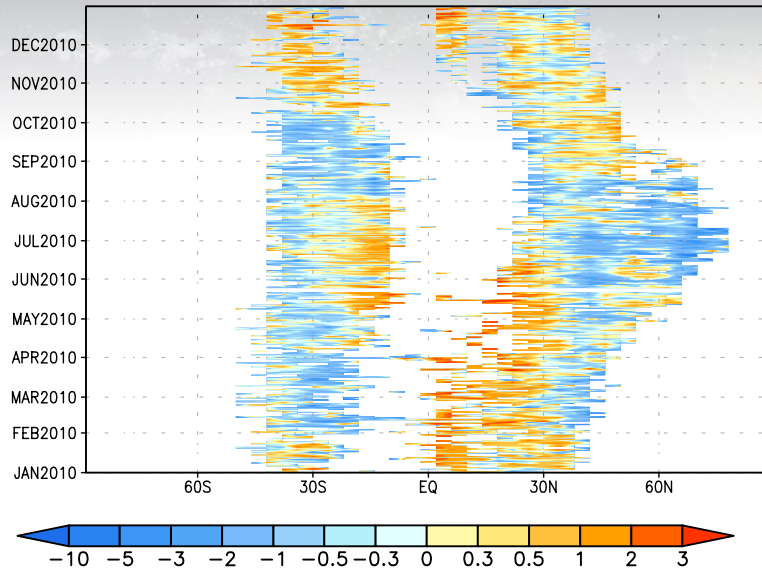
posterior–prior (April–June)



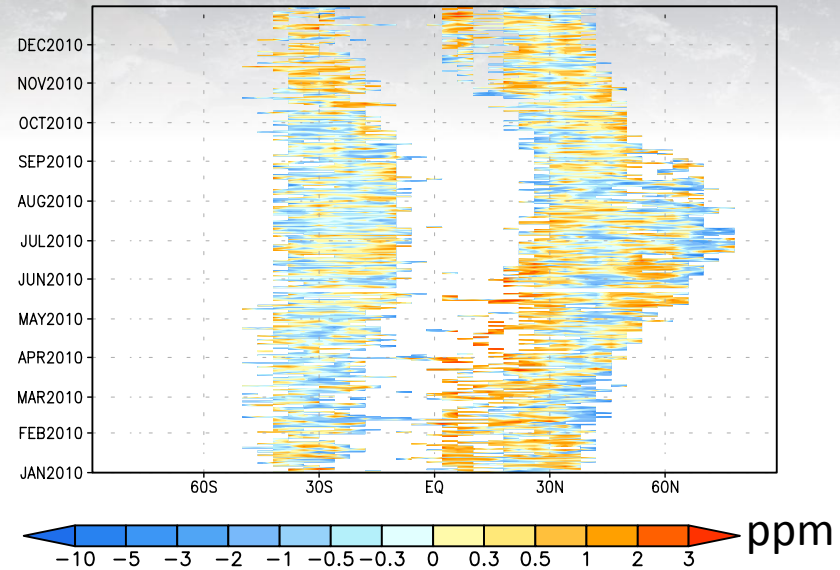


Impact of spatial sampling

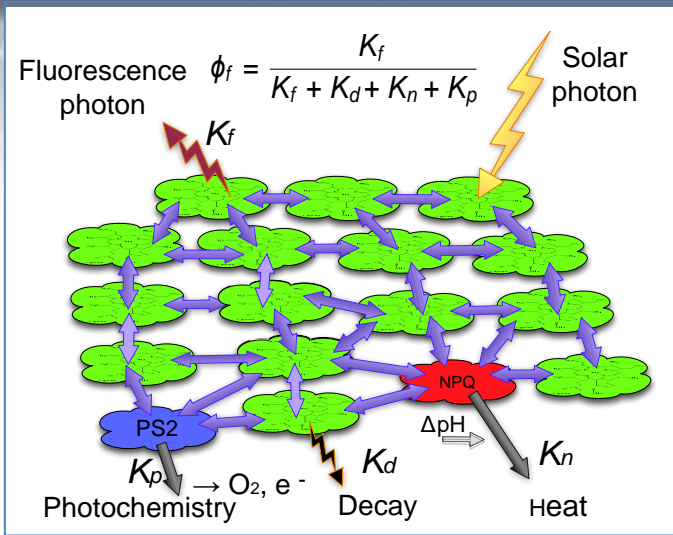
$y-H(x_a)$ (prior flux)



$y-H(x')$ (posterior flux)



- Residual difference (obs-model) shows a strong meridional shift during NH summer.
- Tropical sampling driven by the ITCZ
- Large parts of the world are not observed
 - Southern Hemisphere
 - Northern Hemisphere during Winter and Fall
- Mean residual difference markedly reduced over the year.
- Pattern of differences largely the same
 - Over correcting at mid-high latitudes in the NH during summer time;

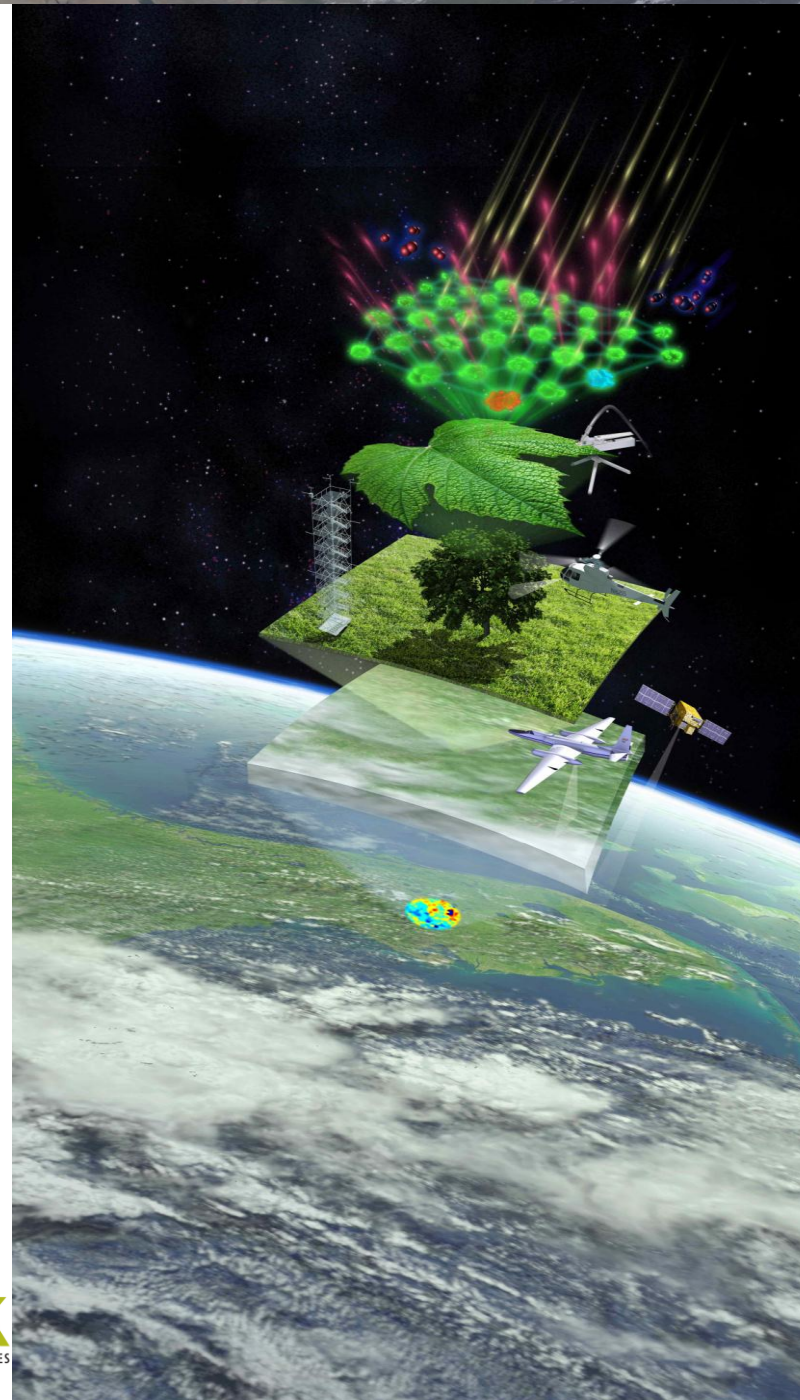


Solar induced Chlorophyll Fluorescence (SIF) is a direct by-product of photosynthesis \rightarrow unique dynamic proxy for gross primary production GPP.

$$SIF = PAR \cdot f_{PAR} \cdot j_f$$

$$GPP = SIF \cdot j_p / j_f$$

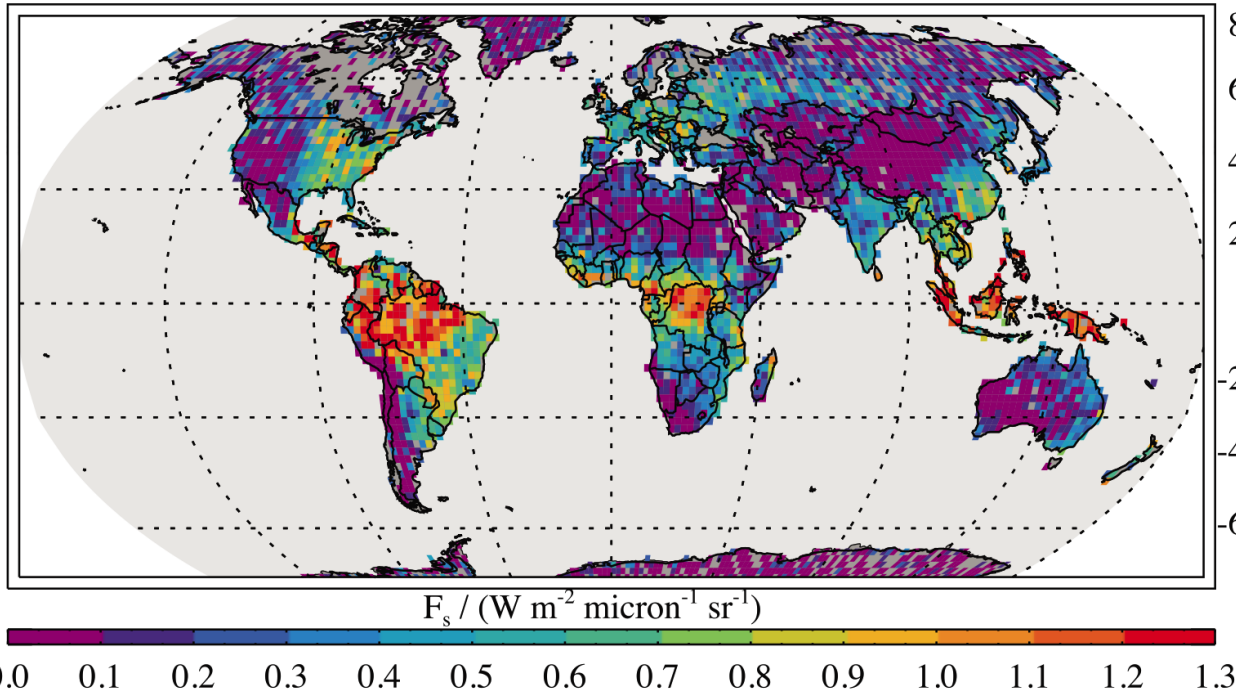
New Methods for Measurements of Photosynthesis from Space!





Planetary photosynthesis

A Chlorophyll a fluorescence at 755 nm, June 2009 through May 2010 average



B Timeseries

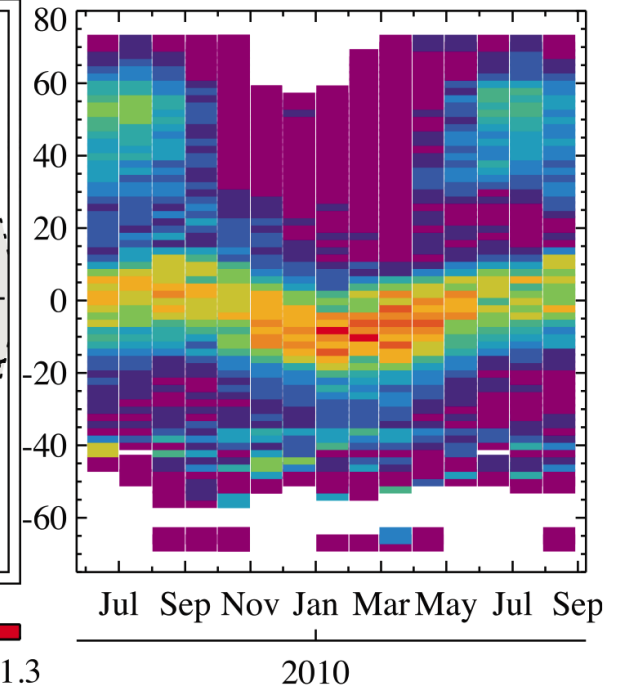


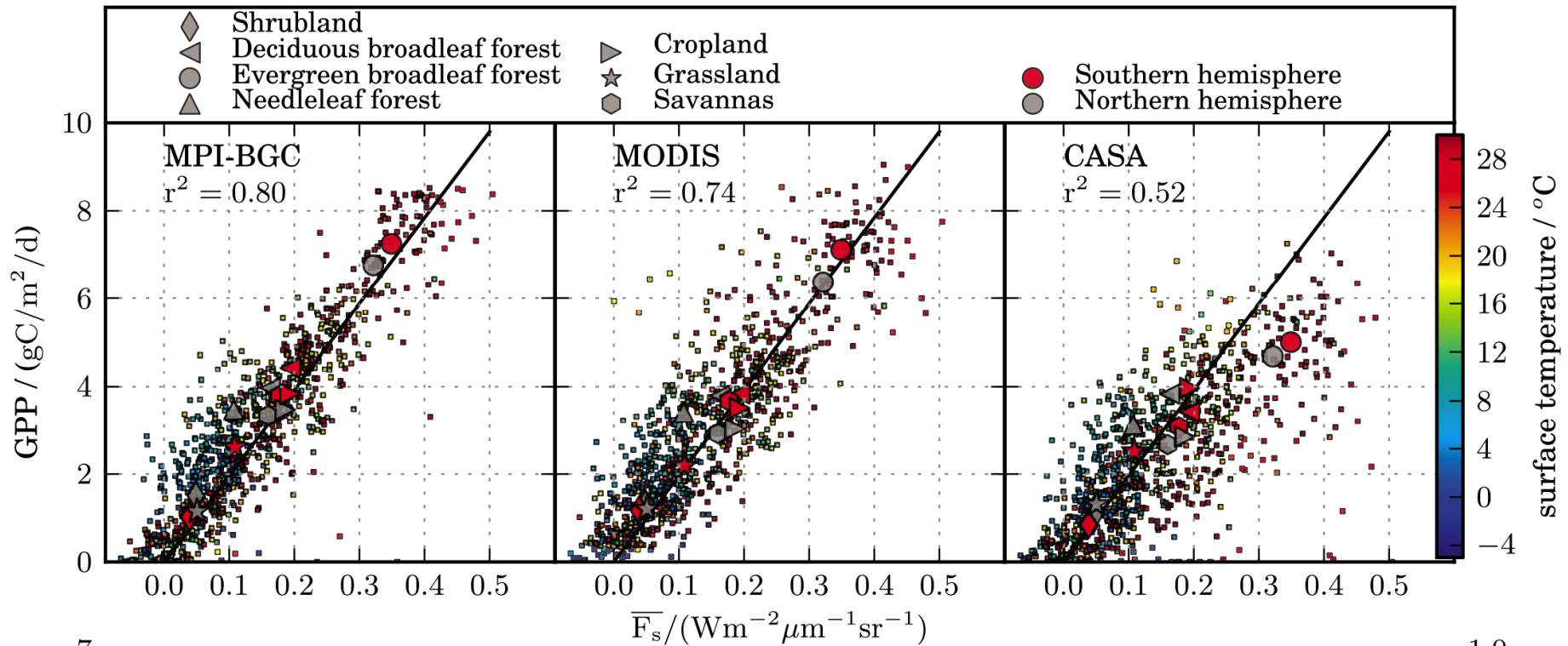
Figure 1. (a) Annual average (June 2009 through May 2010) of retrieved chlorophyll-a fluorescence at 755 nm on a $2^\circ \times 2^\circ$ grid. Only grid-boxes with more than 15 soundings constituting the average are displayed. (b) Latitudinal monthly averages of chlorophyll fluorescence from June 2009 through end of August 2010.

Frankenberg *et al*, 2011

Fluorescence can be measured from GOSAT, GOME-2, and soon OCO-2



Covariation with GPP



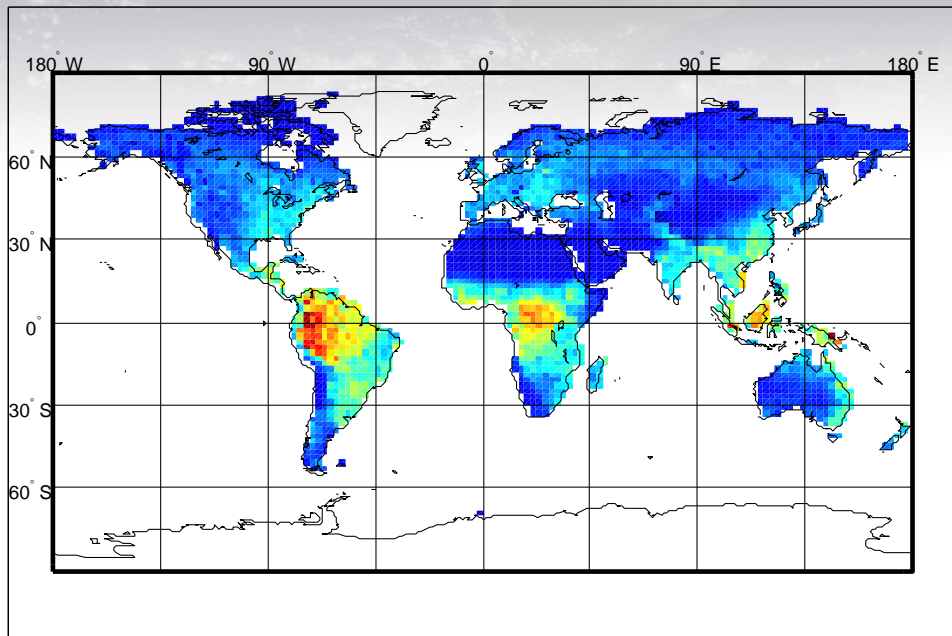
Frankenberg *et al*, 2011

Comparisons with MPI-BGC point to the proportionality of GPP to fluorescence.



Constraints on GPP from SIF

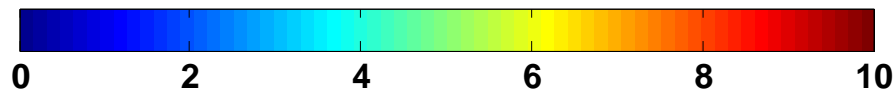
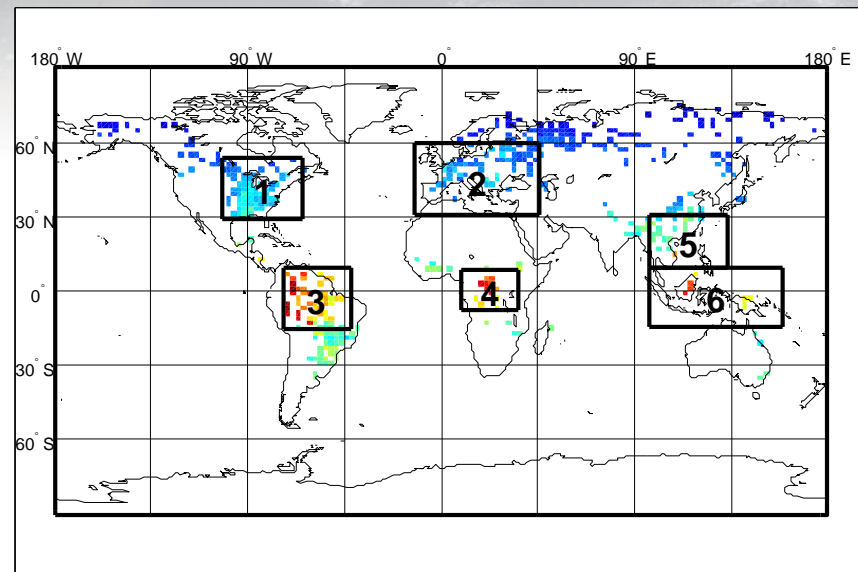
G-opt



Parazoo et al, *in preparation*

gC/m²/day

G-opt (GPP > zonal mean and abs(dBeta) > 5)



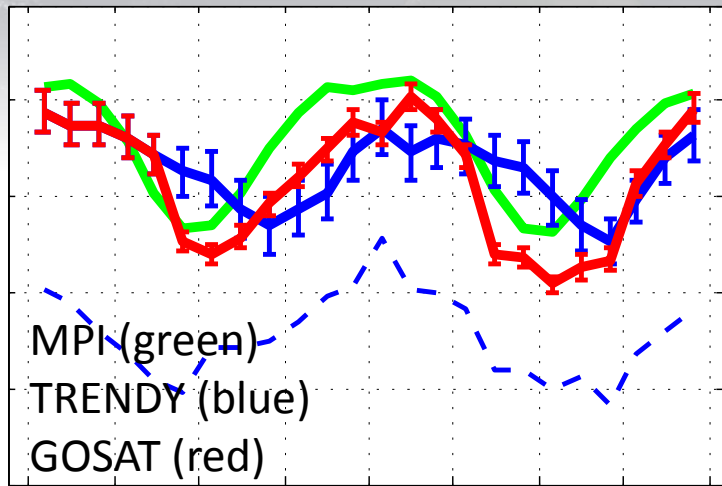
$$\min_{\mathbf{x}_0} C(\mathbf{x}) = \{ (\mathbf{y} - \mathbf{F}(\mathbf{x}))^\top \mathbf{S}_n^{-1} (\mathbf{y} - \mathbf{F}(\mathbf{x})) + (\mathbf{x} - \mathbf{x}_a)^\top \mathbf{S}_a^{-1} (\mathbf{x} - \mathbf{x}_a) \}$$

- Prior distribution from the TRENDY Models
- Accounts for GOSAT sampling, clouds cover, and precision
- Regions with high error reduction relative to inter-model spread also have high GPP

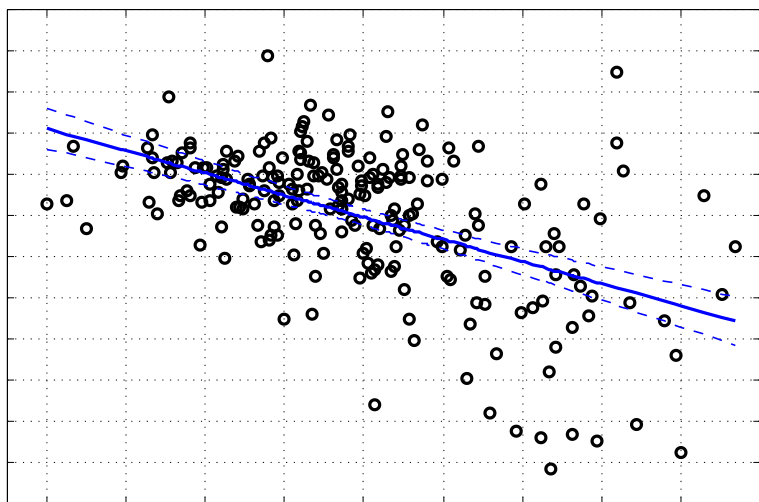


Connecting GPP to NEE

GPP ($gC\ m^{-2}\ day^{-1}$)

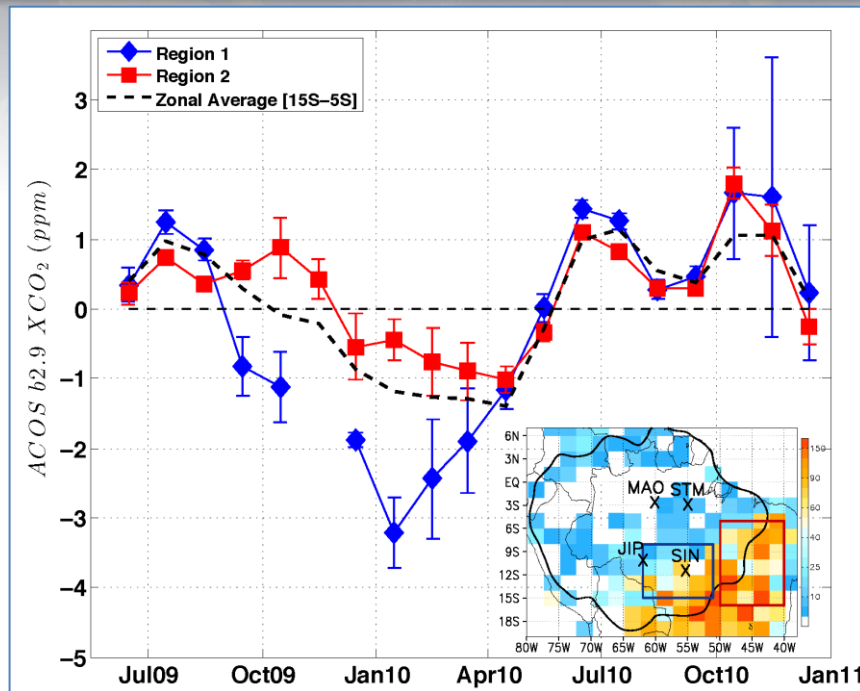


ACOS b2.9 XCO₂ (ppm)



$$GPP (gC\ m^{-2}\ d^{-1}) = 16.28 * SIF (W\ m^{-2}\ micron^{-1}\ sr^{-1})$$

Parazoo et al, GRL 2013



GPP estimates from GOSAT has an earlier draw down in July 2009 and a dramatically weaker GPP in July 2010 than TRENDY

Significant differences in the seasonal cycle of xCO₂ between the tropical transitional forests (TTF) and the cerrado eco-system

Local GPP can explain a significant fraction of xCO₂ variability in TTF



Conclusions

- Quantifying the spatial drivers of climate forcing requires an integrated approach of data, model, and assimilation across the entire carbon cycle.
- Preliminary estimates indicate large-scale zonal and meridional redistribution of carbon uptake relative to the a prior carbon budget
 - Tropical changes appear to be related to biomass burning
 - Northern hemispheric redistribution is potentially related to GOSAT sampling
- The combination of fluorescence-derived GPP and eco-system model estimates show significant variations in sensitive eco-system regions.
- The combination of xCO₂ and fluorescence shows that the CO₂ seasonal cycle in the tropical transitional forests are strongly influence by local GPP.
- **CMS in the context of carbon-climate**
 - The CMS is a carbon cycle reanalysis system that can benchmark CMIP5/CMIP6 carbon-climate models.
 - CMS with new satellites: OCO-2, OCO-3, SMAP, BIOMASS, etc. could provide the required sensitivity to detect and attribute the onset of carbon-climate feedbacks
 - Patterns of flux response diagnosed from CMS to patterns of environmental forcing will provide a powerful resource for finding emergent relationships between present day bias and future response.
- More information at <http://carbon.nasa.gov> and <http://cmsflux.jpl.nasa.gov>



BACKUP



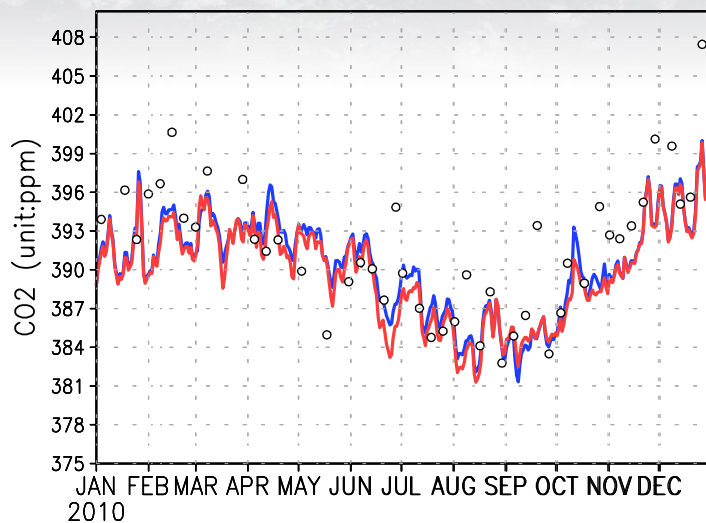
Comparison to surface data

(red: posterior; blue: prior, black: obs)

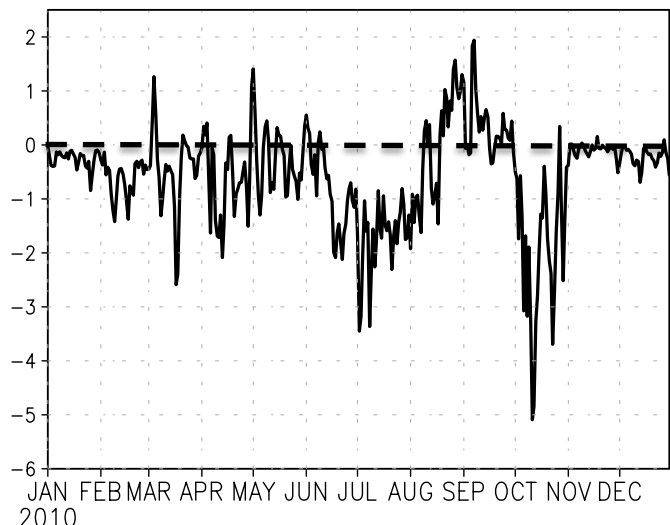
Centro de Investigacion de la Baja

Atmosfera, Spain

name=CIB,lat=41.81,lon=-4.93

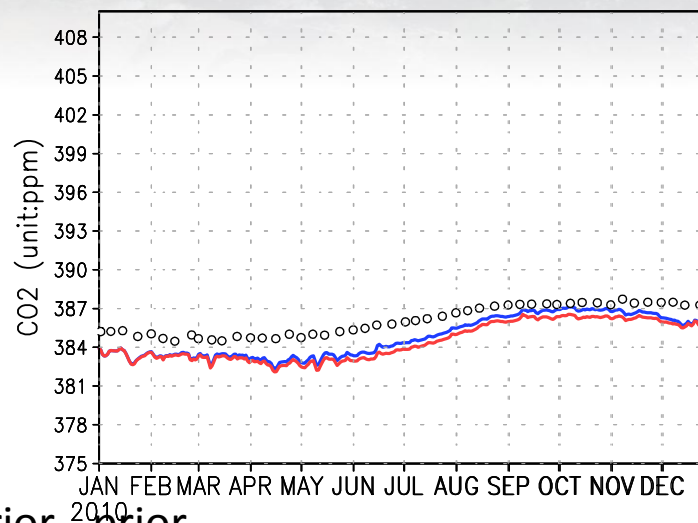


name=CIB,lat=41.81,lon=-4.93

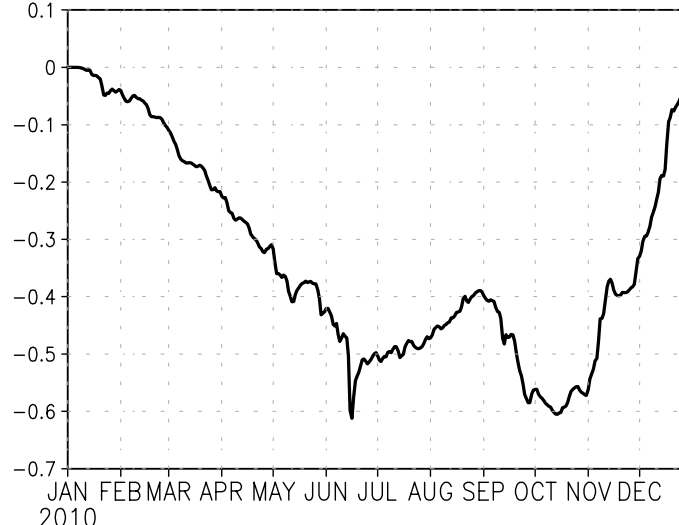


South Pole, Antarctica, US

name=SPO,lat=-89.98,lon=-24.8



name=SPO,lat=-89.98,lon=-24.8



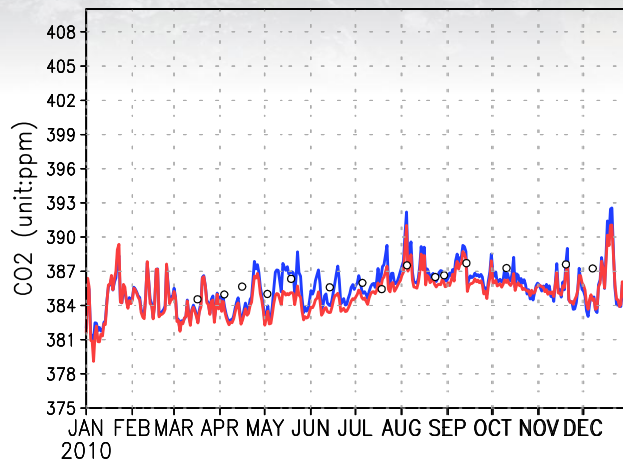
Posterior - prior



Comparison to surface data

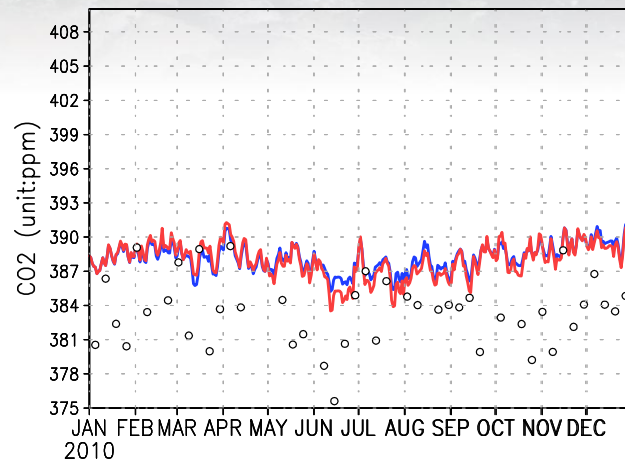
Baring Head Station, New Zealand,

name=BHD,lat=-41.41,lon=174.87

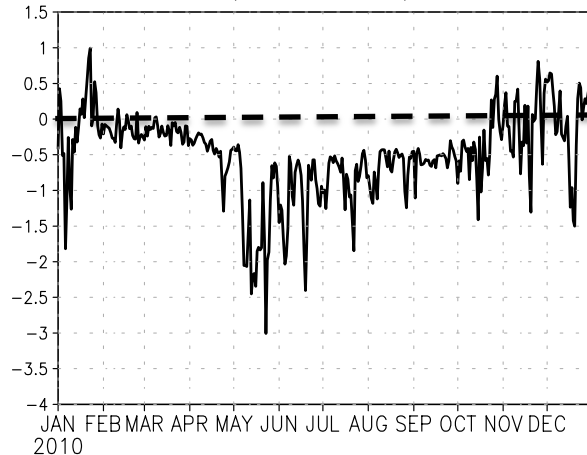


Bukit Kototabang, Indonesia

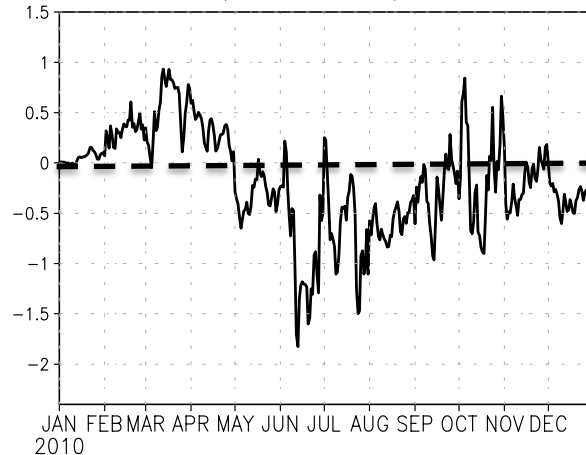
name=BKT,lat=-0.202,lon=100.318



name=BHD,lat=-41.41,lon=174.87



name=BKT,lat=-0.202,lon=100.318

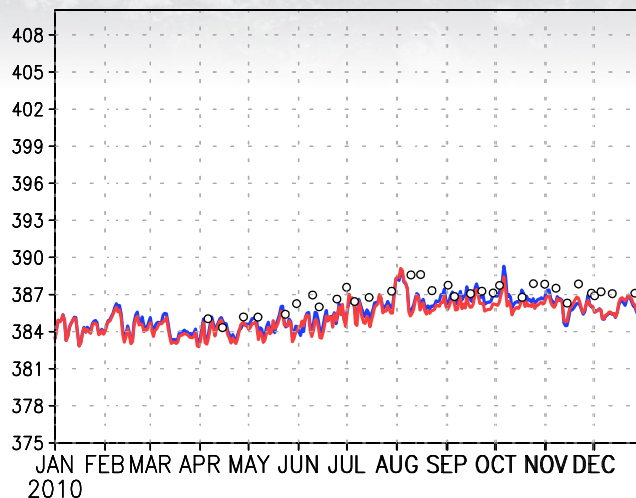




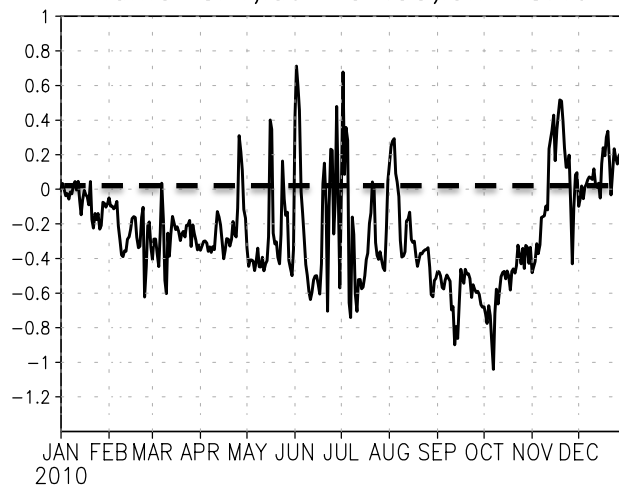
Comparison to surface data

Cape point, South Africa

name=CPT,lat=-34.35,lon=18.49

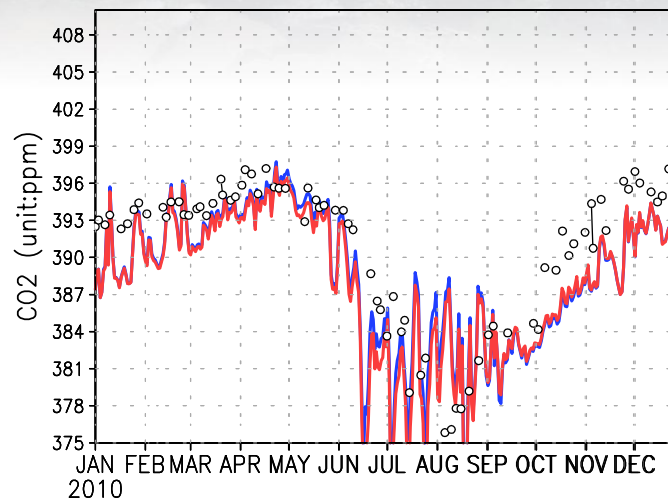


name=CPT,lat=-34.35,lon=18.49

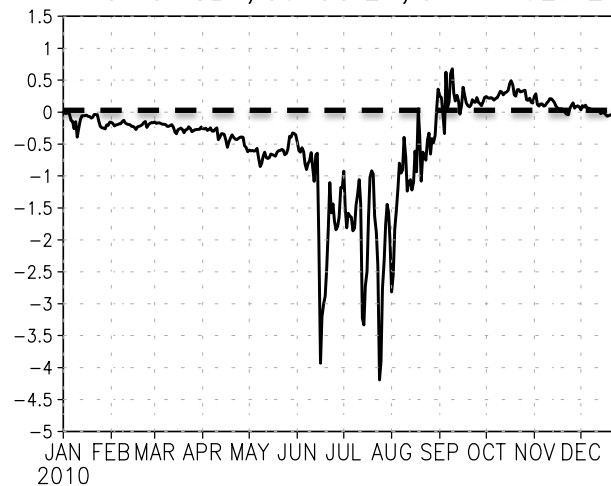


Cold Bay, Alaska, US

name=CBA,lat=55.21,lon=-162.72

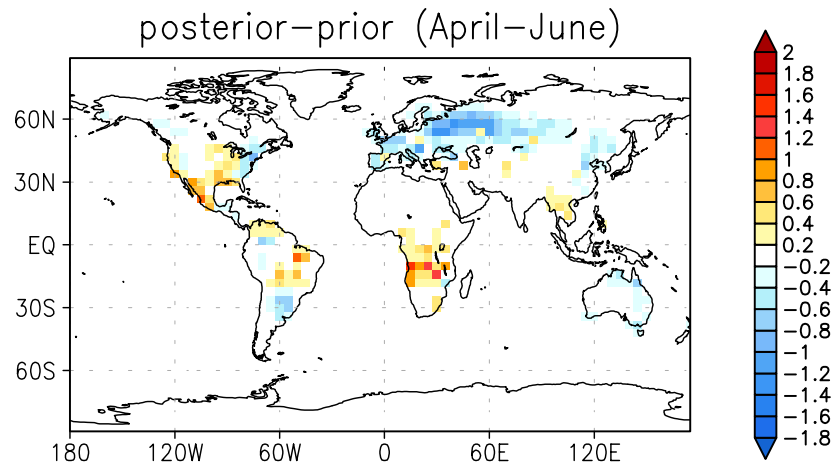
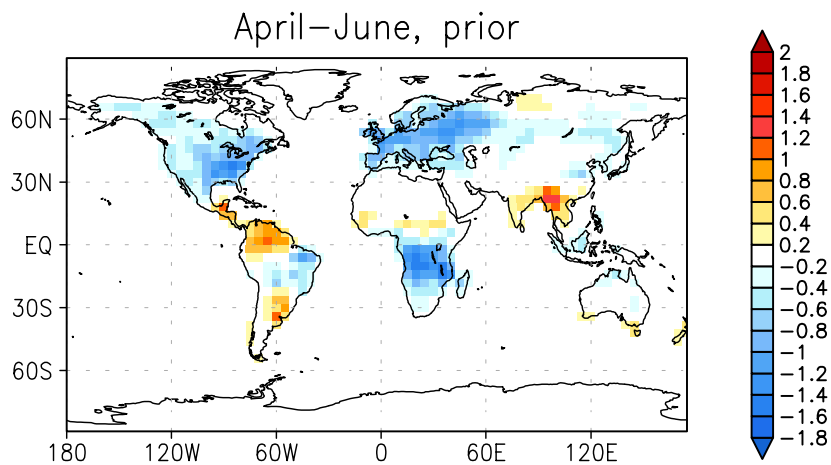
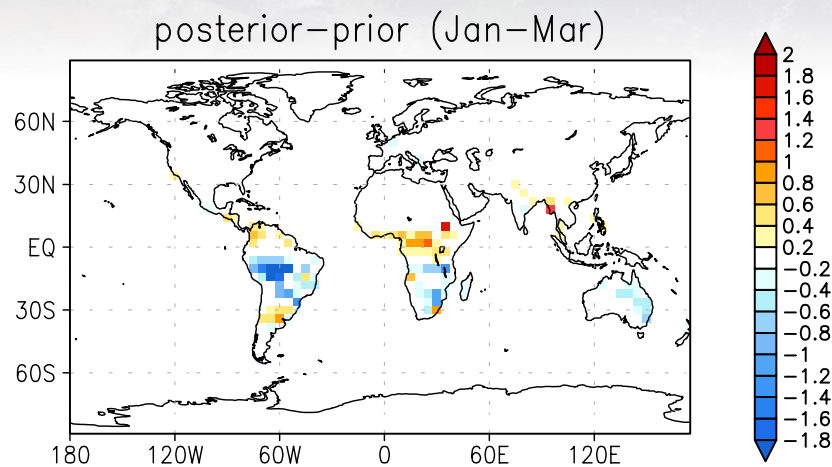
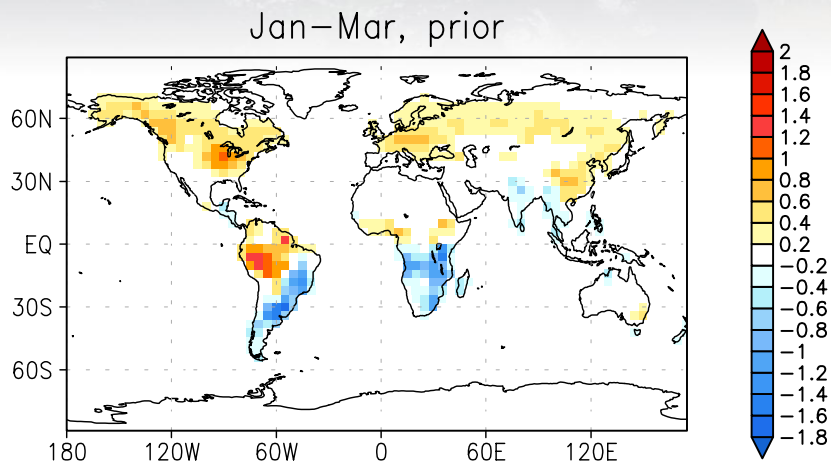


name=CBA,lat=55.21,lon=-162.72





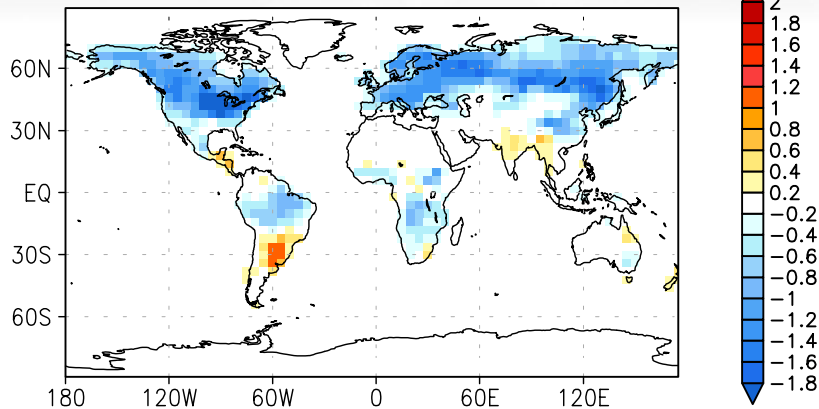
Seasonal prior flux (left panels) and the difference between posterior and prior fluxes



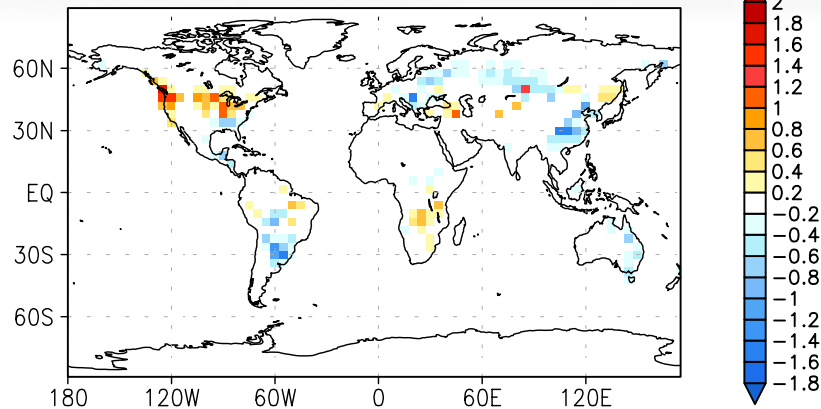


Seasonal prior flux (left panels) and the difference between posterior and prior fluxes

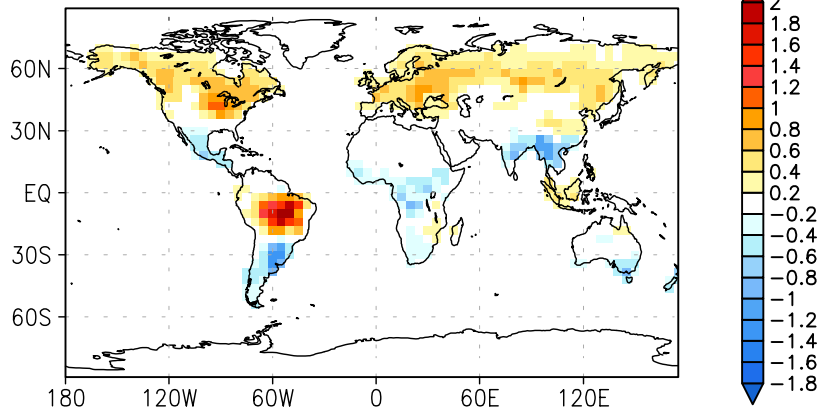
July–Sep, prior



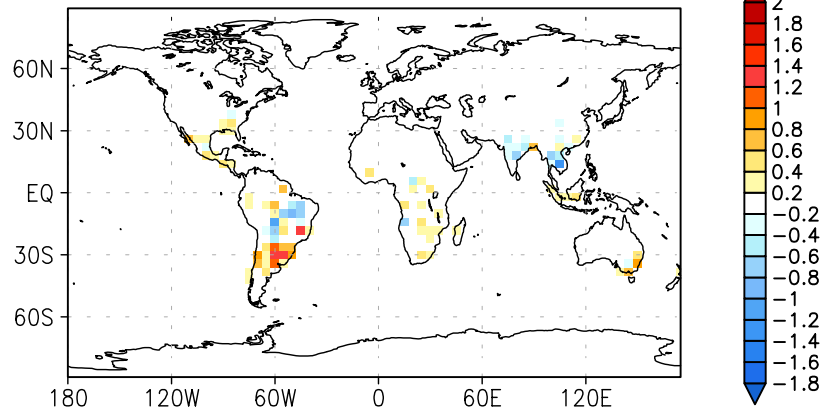
posterior–prior(July–Sep)



Oct–Dec, prior



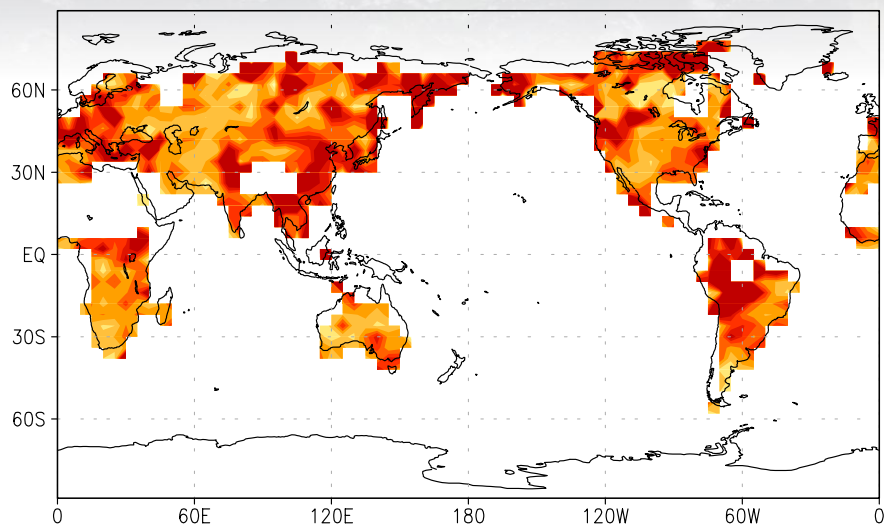
posterior–prior(Oct–Dec)



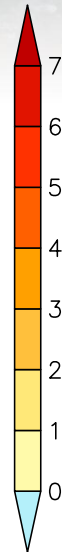


Impact of sampling frequency

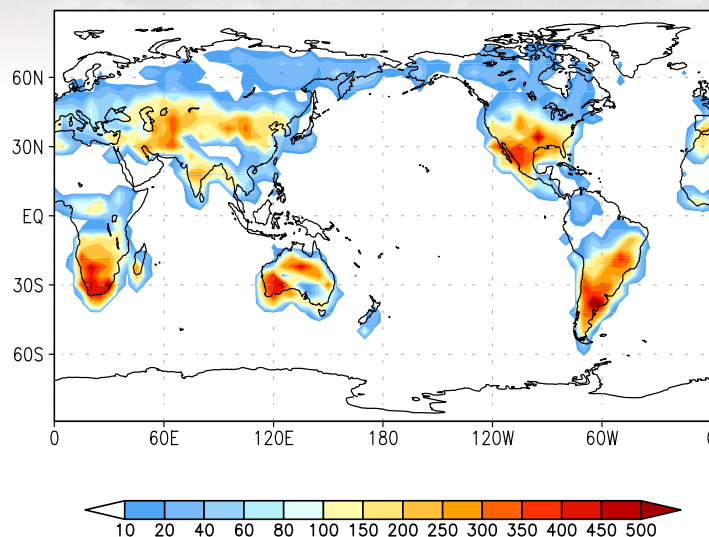
$(y-h(x))^2$ divided by the observation error variance



Chi²



annual total number of observations



- The locations with high chi-square closely follow the sparse observation locations
- High chi-square is a potential consequence of insufficient sampling.
- Using a small number of samples for attribution could be more vulnerable to model and data error.

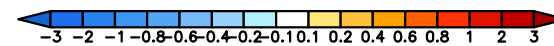
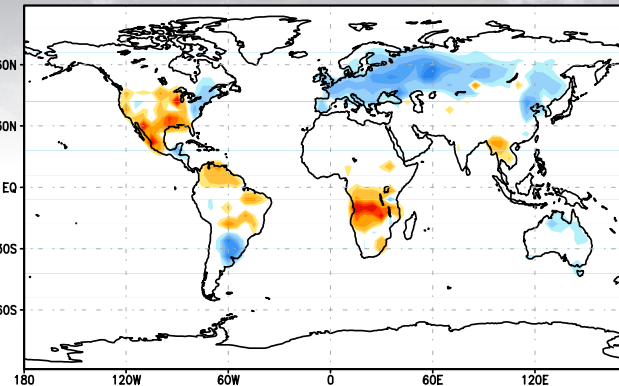
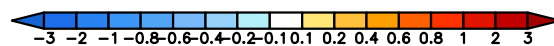
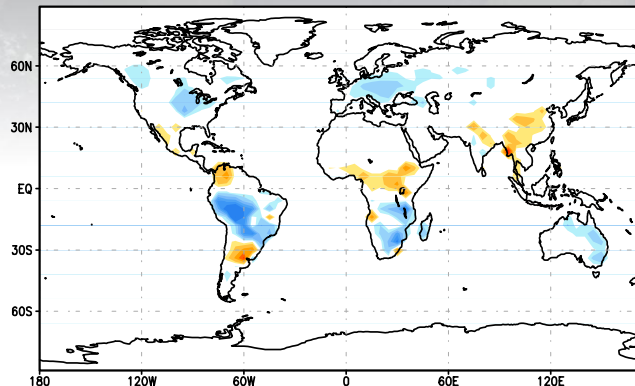


Patterns of change

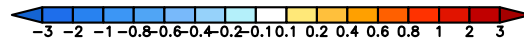
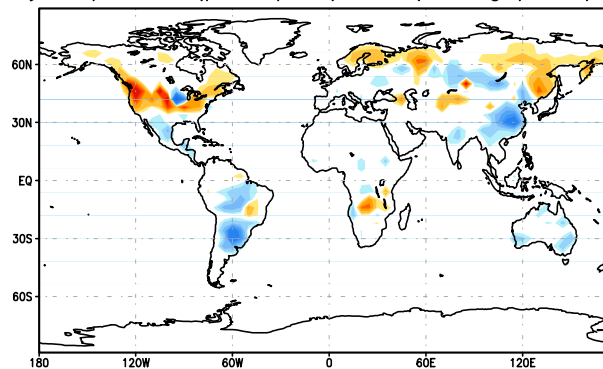
Posterior - prior

The strongest changes happen in the boreal summer over North America and Europe; This is due to both the increase of observations and also the strong variability in the summer.

Jan-Mar 2010 (post-prior) flux (unit: $\text{gC}/\text{m}^2/\text{day}$) | Apr-June 2010 (post-prior) flux (unit: $\text{gC}/\text{m}^2/\text{day}$)



July-Sep 2010 (post-prior) flux (unit: $\text{gC}/\text{m}^2/\text{day}$)



Oct-Dec 2010 (post-prior) flux (unit: $\text{gC}/\text{m}^2/\text{day}$)

